



SINTEF



SeaZero

For an emission-free future

Project Report

Review of Methods for Battery Systems External Short-Circuit Calculations

Sea Zero — Task 2.1 — Deliverable 2.1.1

Author(s)

Daniel Mota

Report Number

2023:00713 — Unrestricted

Client(s)

Members of the Sea Zero Project

Page intentionally left blank.

SINTEF Energi AS

Address:
 Postboks 4761 Torgarden
 7465 Trondheim
 Telephone: +47 40005100
energy.research@sintef.no
 Enterprise Number:
 NO 939 350 675 MVA

KEYWORDS:

Battery systems
 Short-circuit faults

Project Report

Review of Methods for Battery Systems External Short-Circuit Calculations

Sea Zero — Task 2.1 — Deliverable 2.1.1

| | |
|----------------|-------------|
| VERSION | DATE |
| 1.0 | 2023-11-20 |

| |
|------------------|
| AUTHOR(S) |
| Daniel Mota |

| | |
|---|------------------------------|
| CLIENT(S) | CLIENT'S REFERENCE |
| Members of the Sea Zero Project | Task 2.1 - Deliverable 2.1.1 |

| | |
|-----------------------|--|
| PROJECT NUMBER | NUMBER OF PAGES AND ATTACHMENTS |
| 502003620-2 | 43 |

ABSTRACT

This report presents a literature review of methods for calculation of currents in case of short-circuit faults between the external positive and negative terminals of large battery systems. This is the deliverable “D 2.1.1” of the task “T 2.1 Battery systems behaviour during external short circuit” of the [Sea Zero](#) Project Number [340898](#) supported by the [Grønn Platform](#) funding scheme.

| |
|--------------------|
| PREPARED BY |
| Daniel Mota |

SIGNATURE

Daniel Mota

Daniel Mota (Dec 4, 2023 14:43 GMT+1)

| |
|-------------------|
| CHECKED BY |
| Olve Mo |

SIGNATURE

Olve Mo

Olve Mo (Dec 4, 2023 15:35 GMT+1)

| |
|--------------------|
| APPROVED BY |
| Knut Samdal |

SIGNATURE

Knut Samdal

Knut Samdal (Jan 2, 2024 15:26 GMT+1)

COMPANY WITH
 MANAGEMENT SYSTEM
 CERTIFIED BY DNV
[ISO 9001](#) • [ISO 14001](#)
[ISO 45001](#)

| | | | |
|----------------------|-------------------|-----------------------|---------------------------------|
| REPORT NUMBER | ISBN | CLASSIFICATION | CLASSIFICATION THIS PAGE |
| 2023:00713 | 978-82-14-07765-0 | Unrestricted | Unrestricted |

Document History

| VERSION | DATE | VERSION DESCRIPTION |
|---------|------------|---------------------|
| 1.0 | 2023-11-20 | First release |

Contents

| | |
|---|-----------|
| Executive Summary | 5 |
| 1 Introduction | 7 |
| 1.1 Report Outline | 8 |
| 1.2 Scope – External Short-Circuit Faults | 8 |
| 2 Methods for Calculating Short-Circuit Currents (Shorter Version) | 10 |
| 2.1 On the Details of the Model used by Method 1 | 11 |
| 2.1.1 Brief Analysis of the Parameters of the Equivalent Circuit Model | 12 |
| 3 Requirements for Battery Cells and Battery Systems | 14 |
| 3.1 DNV-RU-SHIP Pt.6 Ch.2 [2022] — Propulsion, Power Generation and Auxiliary Systems | 14 |
| 3.1.1 Section 4.2.3 – Cell Tests | 15 |
| 3.1.2 Section 4.2.4 – Battery System Tests | 15 |
| 3.2 IEEE 45.1 [2017] – On Lithium Batteries | 15 |
| 3.3 Next Steps | 16 |
| 4 Studies on Long Duration Short-Circuit Faults | 17 |
| 4.1 Short-Circuit Faults in One Single Cell For Long Periods | 17 |
| 4.2 Identifying Short-Circuit Faults in Single Cells | 18 |
| 4.3 Investigating the Influence of the External Impedance | 19 |
| 4.4 Shape of Long Duration External Short-Circuit Currents | 19 |
| 5 Review of Calculation Methods of Battery Systems External Short-Circuit Currents | 21 |
| 5.1 GE Data Book [1958] – Section 173 | 21 |
| 5.2 Fuses for DC Applications: Where We Stood in 1991 and 1992 | 22 |
| 5.3 Rules of Thumb for the Peak Current | 22 |
| 5.3.1 Twenty-times the Capacity in Ah — Lead-Acid | 23 |
| 5.3.2 Ten Times the 1 min Ampere Rating — Lead Acid | 23 |
| 5.3.3 Ten Times Rated — Lithium-Ion | 23 |
| 5.4 Guides and Recommendations from 1997 to 2020 | 24 |
| 5.4.1 IEEE 399 [1997] — Recommended Practice for Industrial and Commercial Power Systems Analysis (Brown Book) | 24 |
| 5.4.2 IEC 61660-1 [1997] — Short-circuit currents in d.c. auxiliary installations in power plants and substations — Part 1: Calculation of short-circuit currents | 24 |
| 5.4.3 IEEE 1375 [1998] — Guide for the Protection of Stationary Battery Systems | 26 |
| 5.4.4 EPRI TR-100248 [2002] — Stationary Battery Guide: Design, Application, and Maintenance | 28 |
| 5.4.5 IEEE 666 [2007] — Design Guide for Electric Power Service Systems for Generating Stations | 28 |

| | | |
|----------|---|-----------|
| 5.4.6 | IEEE 946 [2020] — Recommended Practice for the Design of DC Power Systems for Stationary Applications | 28 |
| 5.5 | Selection of Publications that Performed Short-Circuit Faults | 28 |
| 5.5.1 | Gerner et al. [2003]: Calculated vs. Measured Short-Circuit Currents | 28 |
| 5.5.2 | Smith et al. [2009]: Sixteen 18650 Lithium-ion Cells Connected in Parallel | 31 |
| 5.5.3 | Satake et al. [2014]: Guide for DC Breakers | 31 |
| 5.5.4 | Gunther et al. [2017]: Tests on Lead-Acid Strings | 31 |
| 5.5.5 | Kriston et al. [2017]: Destructive Tests of Lithium-Ion Pouch Cells | 32 |
| 5.6 | On State of Charge | 33 |
| 6 | Short-Circuit Test Rigs | 35 |
| 6.1 | Simple Rigs for Testing Single Cells | 35 |
| 6.2 | String of VRLA batteries — Gerner et al. [2003] | 35 |
| 6.3 | Automotive Cells — Conte et al. [2009] | 36 |
| 6.4 | Large Lead-Acid Strings — Gunther et al. [2017] | 36 |
| 6.5 | Variable External Short-Circuit Resistance — Jung et al. [2022] | 37 |
| 7 | Conclusion | 39 |
| | Abbreviations and Acronyms | 40 |
| | Bibliography | 41 |

ATTACHMENTS

None

Executive Summary

Increasingly larger battery systems are being incorporated into maritime vessels. As these systems continue to grow in size, their impact on short-circuit currents within the vessels' power systems becomes more relevant. Short-circuit faults pose threats of battery thermal runaway, as well as flammable or toxic off-gas release. Cables and conductors can be vaporized by short-circuit currents provided by modern large battery systems. Poorly sized protection devices and improper selectivity schemes can lead to catastrophic failures. Consequently, the ability of accurately predicting worst-case short-circuit currents from battery systems is vital to ensure the safe operation of the vessel's power system.

Testing the battery system's building blocks and scaling up the results is a promising alternative to performing actual short-circuit tests in each new delivery of a large system. However, even if distinct battery systems from the same manufacturer may share common building blocks (such as battery cells or packs), each new delivery can be different from its predecessors. Therefore, a methodology for estimating real-life short-circuit currents from reduced scale tests is needed. The [Sea Zero](#) project aims to establish a verified methodology for using the results from short-circuit tests on battery modules to calculate the expected short-circuit currents for full battery packs and full battery systems.

As a first step, this report presents the results of a literature survey carried out to identify possible existing methods, standards, or recommendations. In this document, we classify the available methods for calculating the external short-current current supplied by battery cells and systems into two main categories that are relevant to the [Sea Zero](#) project: **(1) empirical electric-equivalent model** of a voltage behind an impedance representing the whole battery system; **(2) empirical equations** describing the rising and decaying phases of the short-circuit current. A third category based on analytical and multi-physics approaches is useful for investigating the internal processes of single battery cells, as well as for developing new chemistries or materials. These analytical methods are, however, impractical to scale up to large battery systems.

Both methods (1) and (2) named previously rely on estimating electric-equivalent parameters for the whole battery system. The level of detail with which the system is modeled varies among different authors. In some cases, only resistive-inductive elements are used. Parallel resistive-capacitive elements are considered in other cases. Temperature and [state of charge](#) dependency may also be taken into account. Results of actual short-circuit tests presented in the scientific literature were digitized with image identification techniques, plotted, and analyzed in this report. Many authors were able to properly model with simple resistive-inductive elements the results obtained with short-circuit tests of battery cells connected in series or in parallel. However, in one case, the models obtained from tests with one single module could not be matched to the results obtained with a string of forty modules in series. It is worth remarking that, due to their vital role in a pragmatic approach to determine short-circuit currents in large battery systems, a chapter of this document is dedicated to describing relevant laboratory setups employed by different authors in the scientific literature.

For summarizing the results of our research, we repeat a relatively common statement present in the scientific literature during the last three decades: "*methods for protection and short-circuit calculation of DC systems are not well established.*" Within the [Sea Zero](#) project, a thorough approach will be necessary for properly forecasting the fault currents supplied by large battery systems based on the results from laboratory tests of the system's building blocks. In addition to the proper scaling and matching test rigs, special attention will have to be given to large scale phenomena that might not be observable during the small scale tests.

Page intentionally left blank.

Chapter 1

Introduction

Increasingly larger battery systems are being incorporated into maritime vessels. As these systems continue to grow in size, their impact on short-circuit currents within the vessel's power grid becomes more pronounced. Consequently, the ability to accurately forecast worst-case short-circuit currents from battery systems is vital to ensure that the vessel's power system is optimally sized to handle the fault currents as well as thermal and mechanical stresses. Moreover, it allows the suitable selection of protection equipment that can limit and break the short-circuit currents in a way that isolates the faults without unnecessary disconnection of equipment, thus, maintaining selectivity.

This report presents a literature review on existing methods for calculating the current supplied by a battery system to a short-circuit fault between the system's external positive and negative terminals. The ability to calculate short-circuit fault currents is important for the following reasons:

- It sets the requirements to busbars, cables, and other components carrying fault currents.
- It provides inputs to the selection and coordination of protective devices, as for example:
 - required interruption time,
 - current limiting ability,
 - selectivity between protection devices.

Battery systems are typically equipped with integrated short-circuit protection devices (fuses). However, these internal protection devices do not act instantaneously. Consequently, the cables and busbars that link battery racks and connect the system to the vessel's grid must be engineered to endure the resulting temperature rise and mechanical stresses induced by the short-circuit currents which are provided by the batteries until the protection devices are able to isolate the fault. This applies to the vessel's DC distribution system itself, demanding a careful evaluation of the temperature rise and mechanical forces caused by the battery system's contribution to a short-circuit fault.

The determination of short-circuit current contributions from battery systems is contingent upon various factors. These include, for instance, cell chemistry, [state of charge \(SoC\)](#), temperature, and built-in protection features. Additionally, the magnitudes of fault currents are highly dependent on the specific topology of the battery system, in other words, the number of cells in parallel and series in battery packs, the number of packs in a string, and the number of strings in parallel. Moreover, the [state of health \(SoH\)](#) of the battery packs can also determine the magnitude of short-circuit currents provided by the system.

Conducting actual short-circuit tests in a large battery system might not be economically feasible. Instead, a pragmatic approach could consist of running tests on the system's building blocks as a way to estimate the short-circuit currents for the complete system. It's important to highlight that even if distinct battery systems from the same manufacturer share common building blocks (such as battery cells or packs), each new delivery could be different from its predecessors. Therefore, a methodology for calculating short-circuit currents is needed. The approach investigated in the [Sea Zero](#) project aims to establish a verified methodology for using test results from short-circuit tests on battery modules to calculate expected short-circuit currents for full bat-

tery packs and full battery systems. As a first step, a literature survey is carried out to identify possible existing methods, standards, or recommendations. This document presents the results of this survey.

1.1 Report Outline

- [Chapter 1 – Introduction](#): this chapter.
- [Chapter 2 – Methods for Calculating Short-Circuit Currents \(Shorter Version\)](#): a summarized version of the short-circuit calculation methods described in international standards and employed by several authors. If you do not have time for the longer literature review on [chapter 5](#), read at least [chapter 2](#).
- [Chapter 3 – Requirements for Battery Cells and Battery Systems](#): a summary of the requirements in international standards for batteries and battery systems.
- [Chapter 4 – Studies on Long Duration Short-Circuit Faults](#): a collection of relevant references which focused mainly long duration faults.
- [Chapter 5 – Review of Calculation Methods of Battery Systems External Short-Circuit Currents](#): available methods are explained in a chronological order.
- [Chapter 6 – Short-Circuit Test Rigs](#): we discuss relevant examples of laboratory setups for testing small and large battery systems.
- [Chapter 7 – Conclusion](#): our final remarks to this report.

1.2 Scope – External Short-Circuit Faults

It is fairly common in the literature to designate as “external” any fault that occurs outside a battery cell. In this report, we focus on short-circuit faults that happen **outside the battery system**, as indicated in red in [figure 1.1](#). This means that the system fuses only have to interrupt the currents supplied by the battery modules and do not have to interrupt currents supplied by external devices connected to the DC system as, for example, chargers, converters, and capacitors.

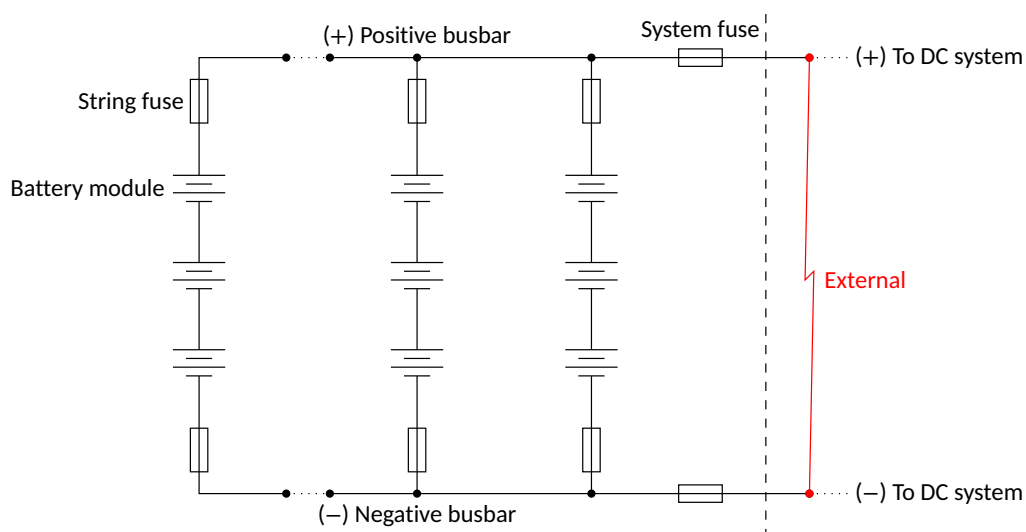


Figure 1.1 | External short circuits.

An external short circuit causes a rapid discharge of the battery and poses threats of thermal runaway, as well as flammable or toxic off-gas release. Electrical protections such as fuses and breakers are the key to preventing this type of failure [Helgesen, 2019]. However, sizing the system fuses and the string fuses in the battery system to **selectively interrupt internal short-circuit currents** would demand the estimation of external contributions from converters and capacitors in the DC system. This is considered **outside the scope** of this report.

A DISCLAIMER ON LEAD-ACID LITERATURE

We believe that the decades-long available literature on lead-acid batteries can provide valuable insights for the [Sea Zero](#) project. Short-circuit current calculation methods based on voltage behind impedance are fundamentally the same across different battery chemistries. Moreover, the challenges of sizing electrical components for a short-circuit test rig are similar for both large lead-acid and lithium-ion batteries.

Chapter 2

Methods for Calculating Short-Circuit Currents (Shorter Version)

After an extensive literature research, we were able to categorize the available methods for calculating the external short-circuit current supplied by battery cells and systems into three main categories:

Method 1 — Empirical aggregated electric-equivalent model of a voltage behind an impedance representing the whole battery system.

Approaches based on [method 1](#) are widely seen in the literature. The level of detail employed by different authors for describing the voltage-behind-impedance models varies considerably. More on this method will be presented in [chapter 5](#). A summarized discussion is, nevertheless, provided in [section 2.1](#).

Method 2 — Empirical equations for describing the rising and decaying phases of the short-circuit current.

This method starts from an aggregated resistive-inductive description of the whole battery system. It then derives certain empirical factors that are used to describe the expected behavior of the short-circuit current. Approaches based on [method 2](#), mainly derived from [IEC 61660-1 \[1997\]](#), will be analyzed in more detail in [chapter 5](#).

Method 3 — Analytical approaches in different time scales that include, for example, electrochemical kinetics and transport phenomena, thermal modeling, and multi-physics coupled models.

Approaches based on [method 3](#) are better suited to investigate the performance of existing cells and develop new chemistries or materials [[Ramadesigan et al., 2012](#)]. They are also typically employed to evaluate the consequences of internal short-circuit faults, which are more complex to address than external ones, as well as predicting thermal runaway [[Abada et al., 2016](#); [Chen et al., 2016](#)]. In some cases, these approaches may even be used to calculate external short-circuit currents, as for instance in [Zavalis et al. \[2012\]](#). However, [Zavalis et al.](#) limited their study to one single cell layer as they focused mainly on the internal dynamics due to external short-circuit faults. Another example of short-circuit tests and modeling of one single cell layer is seen in two companion papers by [Rheinfeld et al. \[2018, 2019\]](#). Approaches based on [method 3](#) are difficult to scale for predicting external short-circuit currents for large battery systems. Therefore, they will not be addressed in this document.

KEY TAKEAWAYS

- **Method 1:** electric equivalent circuit with voltage behind impedance, see summary in [section 2.1](#) and details in [chapter 5](#).
- **Method 2:** empirical equations described by [IEC 61660-1 \[1997\]](#), see more in [chapter 5](#).
- **Method 3:** models that are suited to investigate internal cell dynamics, are not easily scalable to large battery systems, and will not be addressed in detail this document.

2.1 On the Details of the Model used by Method 1

The approaches based on [method 1](#) demand the calculation of an equivalent internal voltage for all cells of the system connected in series and parallel, of an equivalent internal battery impedance, and the equivalent total external impedance. Such model is illustrated in [figure 2.1](#). An example of the level of details employed by different authors is shown in [table 2.1](#).

The following remarks can be made about the model in [figure 2.1](#).

- V — **Open-circuit voltage (OCV)**: aggregates the OCVs of all cells of the system. On the cell level, this voltage depends on SoC, SoH, and temperature. On the system level, one may have to take into consideration the different SoCs and temperatures within the complete system. However, the estimation of minimum and maximum levels of short-circuit currents allow for simplifications assuming best or worst conditions for all cells simultaneously.
- R_0 — **Battery resistance**: aggregates the series resistances of all cells combined. Similarly to the OCV, R_0 depends on SoC, SoH, and cell temperature. Notice that, to properly represent the temperature dependency of R_0 during a long duration short-circuit fault, one needs to build thermal models of the cells. However, thermal models are likely not necessary for millisecond transients.
- L_b — **Battery inductance**: represents an aggregated internal inductance of the batteries. Many authors assume that the internal cell inductance is zero. Some authors attribute to L_b the inductance of internal connections between cells in a battery module.
- R_1C_1 — **Battery resistive-capacitive pair**: can be used to represent the polarization effects in the cells. Two RC pairs were used by [Satake et al. \[2014\]](#). The use of Warburg and [constant phase elements \(CPEs\)](#) [[Plett, 2015](#); [Wang et al., 2015](#)] is usually oriented towards online SoH estimation, parameter identification, and detection of permanent short-circuits of cells or modules inside larger systems, as performed by [Yang et al. \[2018\]](#). In many cases, no RC pairs were used at all. It is, nevertheless, important to remark that the values of the components of the R_1C_1 pair are also dependent on temperature and SoC.
- R_sL_s — **System's equivalent resistive-inductive impedance**: aggregates the impedances of the series and parallel connections among the modules and the external terminals of the battery system. It includes small metal connections, short and long busbars, and cables.

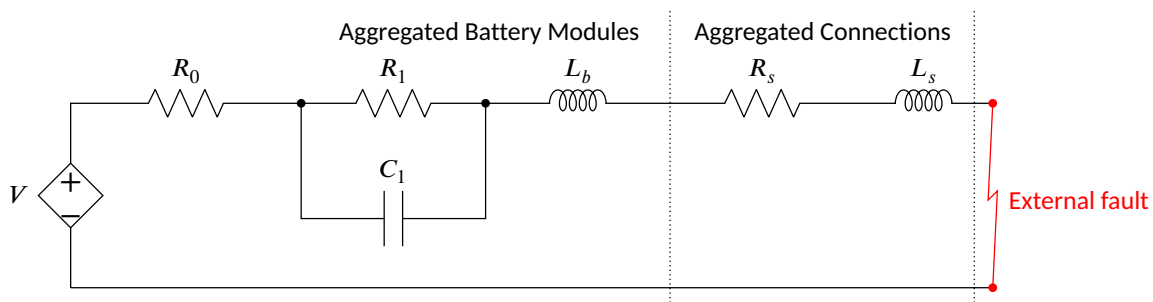


Figure 2.1 | Voltage behind impedance model for calculating external short-circuit currents.

ON THE PARAMETERS OF THE EQUIVALENT CIRCUIT MODEL

- The model parameters vary with SoC, SoH, and temperature.
- Different authors employ different levels of detail for the equivalent model, see [table 2.1](#).

2.1.1 Brief Analysis of the Parameters of the Equivalent Circuit Model

The model in [figure 2.1](#) simplifies the complex interactions among numerous battery cells and their connecting circuits to a second-order RLC system. In this model, the series inductances L_b and L_s limit the steepness of the initial fault current, this effect is illustrated in [figure 2.2a](#). The lower L_s , the steeper is the rate of change of current right after the fault. The maximum attainable peak short-circuit current can be estimated from the OCV divided by the sum of the resistances R_0 and R_s . Notice that R_1 does not initially limit the short-circuit current as the capacitance C_1 serves as a bypass right after the fault. However, as the time passes and depending on the time constant $\tau_{RC} = R_1 C_1$, the resistance R_1 will start limiting the short-circuit current. The influence of $R_1 C_1$ is illustrated in [figure 2.2](#).

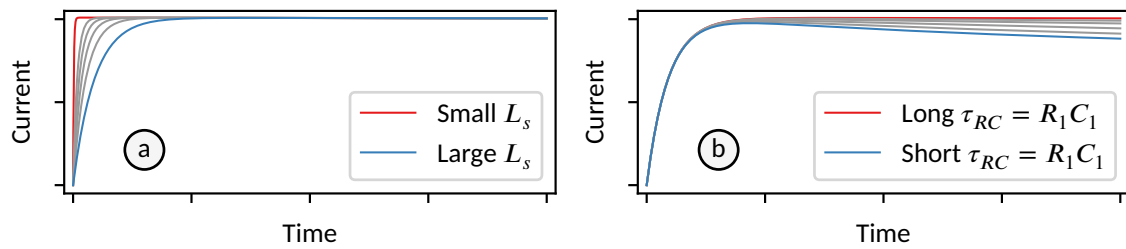


Figure 2.2 | External short-circuit current. (a) Influence of the series inductance L_s on the initial steepness of the fault current. (b) Influence of the $R_1 C_1$ pair in bringing the current down from the initial peak.

Table 2.1: Level of detail employed by different references for the OCV behind impedance model in figure 1.1.

| Reference | OCV V | R_0 | $R_1 C_1$ | L_b | $R_s L_s$ | Comments |
|-------------------------------|---|--|---|---|--|--|
| GE Data Book [1958] | Constant | Constant. Empirical formula with 8h charge current. | Absent | Absent | Present | Lead-acid |
| Willihnganz and Rohner [1959] | Present | Present | Present | Present, approx. 0.1 μH for large lead-acid cells. | Did not discuss external impedance. | Measured elect. equiv. circuit parameters for large lead-acid cells. |
| Berizzi et al. [1994] | Safety factor of 1.05 for charged batteries and 0.9 for discharged. | Multiply known R_0 for charged batteries by 1.7 for discharged ones. | Absent | $L_b = 0.2 \mu\text{H}$ may be used for module with own connectors. | Present | Lead-acid. Reproduces parts of an earlier version of IEC 61660-1 [1997]. |
| IEC 61660-1 [1997] | Constant. Safety factor of 1.05. | Constant. Safety factor of 0.9. | Absent | Absent | Present | Lead-acid. Uses empirical equations (not the simple model) for calculations. |
| IEEE 1375 [1998] | Initial voltage may vary, decreases during prolonged short-circuits | Increases during discharge, increases with age. | Short. lasts for max 15 ms. | Cells internal τ_b from 1 to 3 ms. | Total τ from 5 to 15 ms. Recommends 63% of the peak current for estimating total τ . | Lead-acid and nickel-cadmium |
| Tremblay et al. [2007] | SoC dependent and current dependent. | Constant | Absent | Absent | Absent | Well cited article with a generic electric model for lithium-ion batteries. |
| Smith et al. [2009] | Dependent on SoC. | Dependent on SoC and temperature. | Dependent on SoC and temperature. | Absent | No L_s . Series PTC represented by temperature dependent R_s . | 16 lithium-ion cells in parallel. |
| Satake et al. [2014] | Present | Present | Two pairs of RC in series. Match $R + RC$ impedance characteristics of model and real system. | Absent | Did not discuss $R_s L_s$. | For PV and wind energy. Measured results with similar shape to figure 5.2. |
| Chen et al. [2016] | Polynomial function with parameters from a look-up table | Present | Present | Absent | Absent | Single lithium-ion cell with SoC varying from 10% to 100%. |
| Gunther et al. [2017] | Constant | Constant, but authors admit it is temperature dependent. | Absent | Absent | Constant, but authors admit resistance is temperature dependent. | Matched models to real short-circuit tests on three different battery strings. |
| Lee et al. [2018] | SoC dependent | Age and temperature dependent. | Absent | Absent | Resistive | Inrush calculations for hot swapping of lithium-ion modules. |

Chapter 3

Requirements for Battery Cells and Battery Systems

As a part of the literature review on external short-circuit current calculation, we list the requirements set forth by [DNV-RU-SHIP Pt.6 Ch.2 \[2022\]](#) for battery cells and for battery systems. We also present the recommendations for electrical installations in shipboard-design by [IEEE 45.1 \[2017\]](#).

3.1 [DNV-RU-SHIP Pt.6 Ch.2 \[2022\]](#) — Propulsion, Power Generation and Auxiliary Systems

Table 8 of [DNV-RU-SHIP Pt.6 Ch.2 \[2022\]](#) presents a list of documentation requirements and component certification for lithium-ion battery systems. More specifically on the topic of short circuits, manufacturers must provide documentation regarding:

- The short circuit capacity, which “shall be stated for both maximum (fully charged new battery) and minimum (discharged battery at estimated end of lifetime) capacity”.

Considering the [electrical energy storage \(EES\)](#) system as whole, section 3.2.1.3 of the class notation demands that:

- “An [EES](#) system shall be able to supply the short circuit current necessary to obtain selective tripping of downstream circuit breakers and fuses.”

To guarantee the selectivity between the battery system’s protection devices and the ones placed downstream in the direct current system, manufacturers need to properly estimate maximum and minimum short-circuit currents provided by their battery systems both at the beginning and at the end of their operation lives. Therefore, [state of charge](#) and ageing must be taken into consideration by manufacturers when estimating fault currents.

SELECTIVITY MUST BE GUARANTEED

- Manufacturers must estimate **maximum and minimum short-circuit currents** for fully charged and fully discharged battery systems, both **at the beginning and at the end of operation life**.

In the following subsections, we will present the requirements from [DNV-RU-SHIP Pt.6 Ch.2 \[2022\]](#) regarding cell and system tests, respectively.

3.1.1 Section 4.2.3 – Cell Tests

Section 4.2.3 of [DNV-RU-SHIP Pt.6 Ch.2 \[2022\]](#) points to two standards for testing battery cells, namely [IEC 62619 \[2022\]](#) and [UN 38.3 T-5 \[2019\]](#).

- [IEC 62619 \[2022\]](#) — **Section 7.2.1 – External Short-Circuit Test (Cell or Cell Block)**

About the standard: “specifies requirements and tests for the safe operation of secondary lithium cells and batteries used in industrial applications, including stationary applications.”

Test pass criteria: “Short-circuit between the positive and negative terminals shall not cause fire or explosion.”

Test procedure:

- Fully charged cells stored in ambient temperature of 25 ± 5 °C.
- External short-circuit resistance of 30 ± 10 mΩ.
- Short circuit remains for 6 h or until case temperature drops to 80 % of the maximum reached temperature, whichever happens sooner.

- [UN 38.3 T-5 \[2019\]](#) — **Section 38.3.4.5 Test T.5: External short circuit**

About the manual: “contains criteria, test methods and procedures to be used for the classification of dangerous goods according to the provisions of the ‘United Nations Recommendations on the Transport of Dangerous Goods, Model Regulations’...”

Test pass criteria: “external temperature does not exceed 170 °C and there is no disassembly, no rupture and no fire during the test and within six hours after the test.”

Test procedure:

- Cell or battery should be heated until reaching a homogeneous temperature of 57 ± 4 °C measured on the external case. The heating period should be of at least 12 h for large batteries.
- External short circuit resistance of less than 0.1 Ω.
- Short circuit remains “for at least one hour after the temperature has returned to 57 ± 4 °C, or in case of the large batteries, has decreased by half the maximum temperature increase observed during the test and remains below this value.”
- “The short circuit and cooling down phases shall be conducted at least at ambient temperature.”

Notice that [IEC 62619 \[2022\]](#) and [UN 38.3 T-5 \[2019\]](#) have different requirements for battery temperature before starting the short-circuit test, for total short-circuit resistance, as well as different requirements for stopping and passing the test. It is not within the scope of this report to assess which requirements are better or worse. However, the important take from these requirements is that **cell** in a battery system **must survive longstanding short circuits** between their positive and negative terminals.

3.1.2 Section 4.2.4 – Battery System Tests

Section 4.2.4 of [DNV-RU-SHIP Pt.6 Ch.2 \[2022\]](#) defines a series of routine and type tests for battery systems. Among them, we can mention handling and mitigating propagation of thermal events, overvoltages, overcurrents, overheating, cooling failures, etc. There is, however, **no requirement for an external short-circuit test** for the whole system.

3.2 IEEE 45.1 [2017] – On Lithium Batteries

The complete name of [IEEE 45.1 \[2017\]](#) is “Recommended Practice for Electrical Installations on Shipboard-Design”. This standard is succinct on its recommendations for lithium battery systems. From the standard’s section 11.3.11, we would like to remark the following recommendations.

- Lithium-ion batteries must be procured as a system which include the battery pack, the battery management system, and the charging system.
- The battery and battery system should be protected against overload and short-circuit faults.

Notice that there is no specific recommendation or requirement regarding short-circuit tests of lithium batteries in IEEE 45.1 [2017].

EXTERNAL SHORT-CIRCUIT TESTS AND LARGE BATTERY SYSTEMS

- DNV-RU-SHIP Pt.6 Ch.2 [2022] and IEEE 45.1 [2017] **DO NOT REQUIRE** external short-circuit tests to be performed for a complete large battery system.

3.3 Next Steps

DNV-RU-SHIP Pt.6 Ch.2 [2022], IEC 62619 [2022], and UN 38.3 T-5 [2019] demand that each cell in the battery system must survive without out-gassing or catching fire a longstanding short-circuit fault between the its terminals. In the next chapter, we will discuss references from the last two decades that investigated the consequences of long duration short-circuit faults on the time scales of seconds to minutes and hours.

Chapter 4

Studies on Long Duration Short-Circuit Faults

According to [DNV-RU-SHIP Pt.6 Ch.2 \[2022\]](#), [IEC 62619 \[2022\]](#), and [UN 38.3 T-5 \[2019\]](#), each cell in the battery system is required to survive without out-gassing or catching fire a longstanding short-circuit fault between the cell's terminals. Many authors in the last two decades have investigated the consequences of long duration short-circuit faults on the time scales of seconds to minutes and hours. However, the contribution of several battery modules in parallel can lead to extremely high external fault currents, "vaporization of large conductors is possible" [[Nailen, 1991](#)]. Because of that, designing a large system that withstands long duration external short-circuit faults is not economically viable. Fast acting protection devices such as fuses are necessary for avoiding the catastrophic destruction of batteries, cables, busbars, and power distribution systems. Nevertheless, the practical results obtained by different authors while short-circuiting batteries during seconds and minutes can provide valuable insights for [Sea Zero](#) project. Therefore, we discuss relevant examples from the literature in the following sections.

4.1 Short-Circuit Faults in One Single Cell For Long Periods

[Conte et al. \[2009\]](#) performed short-circuit tests in nine automotive lithium-ion cells, one at a time, employed in hybrid and purely electrical vehicles. The authors described their test setup, see [section 6.3](#), and presented time-domain results of the short-circuit tests in one of their cells (probably one of 40 Ah capacity). The test results are shown in the paper by [Conte et al.](#) with time window of 400 s. The sampling time was not informed, but judging from the graphics, it seems to be on the range of a few tenths to one second. The shape of this long-duration short circuit current will be discussed later in [section 4.4](#).

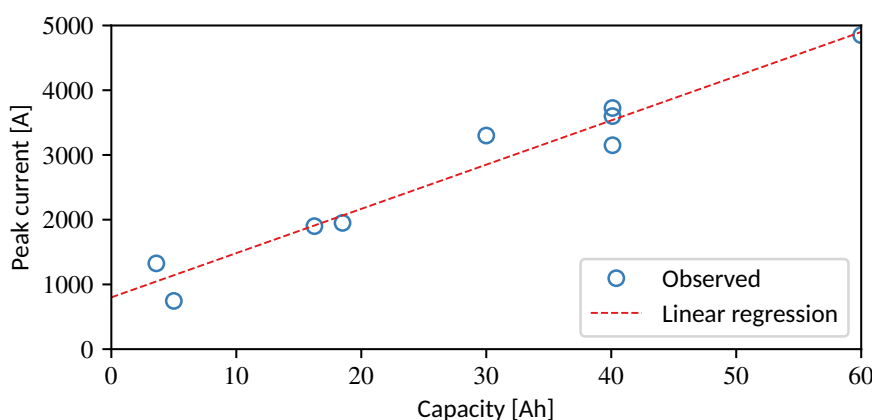


Figure 4.1 | Measured peak short-circuit current versus lithium-ion cell capacity. Data acquired with image identification techniques from the original in [Conte et al. \[2009\]](#).

An interesting result presented by [Conte et al.](#) is a curve with the peak short-circuit current versus the capacity of nine different cells. An approximation of the this curve, obtained with image identification techniques, is shown in [figure 4.1](#). The linear regression curve (dashed red) in [figure 4.1](#) can be represented by an equation. From the charts, **we estimate** that this equation is:

$$I_{\text{peak}} [\text{A}] = 800 [\text{A}] + 68.333 \left[\frac{\text{A}}{\text{Ah}} \right] \times \text{Capacity} [\text{Ah}].$$

It is worth quoting [Conte et al.](#)'s conclusions regarding short-circuit currents in large battery systems:

- “Experience showed that... **A cell that withstands a short circuit test at cell level may fail in a short circuit module or at system level...** The reason is that at cell level the internal capacity of the cell is comparable with the external short circuit wiring resistance... **As soon as the number of cells in series increases and at the same time the short circuit test equipment remains the same, the total internal resistance increase and the resistance of the test equipment gets always more negligible.**”¹

We found other publications that investigated methods for online detection of short-circuit faults in single lithium-ion cells. For the sake of brevity, we decided not to include them all in this report. Nevertheless, to emphasize the time scale of these “long duration faults”, we can mention [Xiong et al. \[2020\]](#), who presented a “fast” method for identifying external short-circuit faults in lithium-ion battery packs that acted “in 3.5 s after their occurrences.” Within the context of the [Sea Zero](#) project, a slow reaction only 3.5 s after an external short-circuit fault may have catastrophic consequences.

Another example of long-term faults is found in [Xia et al. \[2014\]](#), who presented methods for the detection of external short-circuit faults in 18650 1.35 Ah lithium-ion cells based on voltage, current, or temperature measurements. [Xia et al.](#) stated that their methods could be employed to detect faults at an “early stage”. However, the faults performed by these authors lasted for many minutes and were recorded with sampling time of 100 ms. It is worth mentioning that [Xia et al.](#) performed many short-circuit tests with varying SoC from zero to one hundred percent in steps of ten percent, see more in [section 5.6](#). In a continuation of their 2014 paper, [Xia et al. \[2015\]](#) logged their measurement with much shorter sampling times. Notwithstanding, the time scales defined as fast by these authors are not fast enough for the [Sea Zero](#) project.

4.2 Identifying Short-Circuit Faults in Single Cells

Two publications by [Yang et al. \[2018, 2020\]](#) dealt with methods for identifying permanent short-circuits in isolated single cells or in single cells within electrical vehicles batteries composed of multiple strings in parallel with several cells in series. In [Yang et al. \[2018\]](#), fractional-order and first order *RC* modelling with genetic algorithms for parameter identification, associated with with random forest classification methods, were employed to identify external short-circuit faults in lithium-ion cells. This is the only reference found by us that employed CPEs and Warburg elements in conjunction with short-circuit studies. [Yang et al. \[2020\]](#) presented a method using artificial neural network coupled with a three-dimensional thermal modeling of the cells to identify short-circuits faults in single cells within an electric vehicle battery system with parallel strings. The authors affirmed that their method can estimate the cell’s external short-circuit current using only the voltage information, and that the maximum surface temperature of the cell can be estimated without a current or temperature sensor.

The problems analyzed by [Yang et al. \[2018, 2020\]](#) are not directly aligned with the objectives of this report. Firstly, we focus on short-circuit faults that happen outside a battery system with multiple strings composed of many modules in series. Secondly, the short-circuit currents under study in this report will be “easily detectable”. They will either activate protection devices (as expected) or destroy cells and melt conductors (not expected). Notwithstanding, these papers are still mentioned in this report as they present charts of actual short-circuit tests performed in lithium-ion cells under different temperature and SoC. One of the results from [Yang et al. \[2020\]](#) is shown in later [figure 4.2](#).

¹Emphasys given by us.

4.3 Investigating the Influence of the External Impedance

Zhao et al. [2016] performed nail tests and external short-circuit tests in lithium-ion cells. The external short circuits were performed with different resistances (R_s). Zhao et al. noticed that the contact regions between clamps and positive tabs (aluminum) of some batteries “were broken by the concentrated heat” for the lowest range of R_s . This serves as a reminder that the internal connections of a large battery system may inadvertently work as fuses during the fault.

Abaza et al. [2018] presented experimental results obtained with nail perforation and external short-circuit tests of 15Ah cell with six different external resistances (R_s) ranging from 0.562 m Ω to 821 m Ω . Abaza et al. focused only on destructive and long duration faults. The authors included, for instance, a nail in their short-circuit test rig meant for “for cell disposal”. The external short-circuit results presented in the paper show a time window of 40 s. It is not possible to discern the dynamics of the current in the first milliseconds after the fault. In the time scale employed by the authors, the rise time is almost instantaneous. It is nonetheless worth comparing the measured short-circuit currents versus the external resistances:

- $R_s = 0.562 \text{ m}\Omega$, peak short-circuit current above 1000 A.
- $R_s = 24 \text{ m}\Omega$, peak short-circuit current below 200 A.
- $R_s = 501 \text{ m}\Omega$, peak short-circuit current below 10 A.

Jung et al. [2022] assessed the requirements for the total external short-circuit resistance for testing battery cells in regard to the safety of battery energy storage systems. To reiterate the statement “*methods for protection and short-circuit calculation of DC systems are not well established*”, we quote the following passage from Jung et al.:

- “existing evaluation methods performed external short-circuit tests merely targeting cylindrical batteries. In other words, none of the studies carried out so far involved external short circuits in medium- and large-sized batteries”.

Even though the initial rise in the first milliseconds after the short-circuit faults cannot be discerned in any of the charts presented by Jung et al., it is worth quoting an important conclusion from their article:

- “the external short circuit-resistance should be lowered to the standards for EV batteries in order to achieve a meaningful assessment of the battery safety, as the external short-circuit resistance of ESS batteries in the current standards is too high.”

KEY TAKEAWAYS FROM THE AUTHORS WHO STUDIED THE INFLUENCE OF THE EXTERNAL RESISTANCE

- Zhao et al. [2016]: internal devices / cells may inadvertently work as fuses.
- Abada et al. [2016]: have full control of all the test rig’s m Ω impedances.
- Jung et al. [2022]: external short-circuit resistance defined by current standards are too high.

4.4 Shape of Long Duration External Short-Circuit Currents

Figure 4.2 shows examples of the test results acquired with image identification techniques from different authors of the lithium-ion battery literature. For information on the conditions of the tests and for relevant comments, please see table 4.1. The cells tested by Smith et al. [2009] had built-in positive temperature coefficient resistor (PTC) elements to limit the short-circuit current based on the temperature of the cell. This is the cause of the drastic fall in the short-circuit current seen in the solid purple curve in figure 4.2. Conte et al. [2009] did not discuss the reasons why the short-circuit current (solid red) measured by them had a fast decay in less than 3 s to approximately 40 % of the peak. The results from Yang et al. [2020] (solid blue) also feature a relevant decay in the short-circuit current that stabilizes at around 50 %. Notice that the test is stopped at time

27 s. Although not shown in [figure 4.2](#), the results results obtained by [Xia et al. \[2014\]](#) for external short-circuit faults applied to single 18650 cylindrical cells at various *SoCs* are very similar to the ones obtained by [Yang et al. \[2020\]](#). The tests performed by [Jung et al. \[2022\]](#) have the least prominent decay. It is worth remarking that [Jung et al.](#) drove the tests for periods longer than 1000 s.

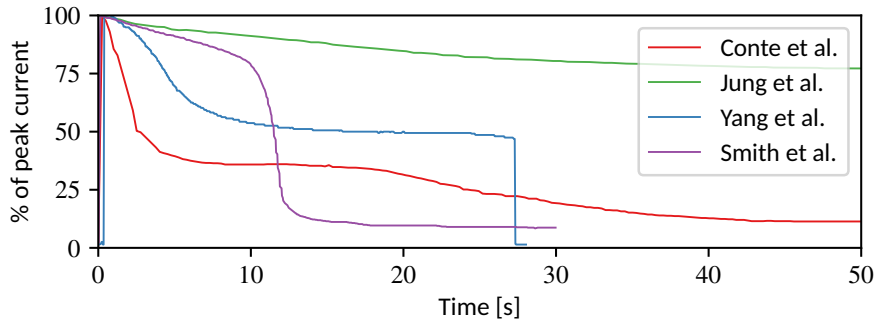






Figure 4.2 | Approximate shape of the measured short-circuit current in lithium-ion modules. Data acquired with image identification techniques from different references. See [table 4.1](#) for more information.

Table 4.1: Legend information for [figure 4.2](#).

| Reference | Battery type | Peak current | Comments |
|---|---|--------------|--|
|  Conte et al. [2009] | Non-specified automotive battery/module, probably of 40 Ah. | 3 kA | Short-circuit resistance not informed. |
|  Jung et al. [2022] | Non-specified prismatic cell, pre-fault OCV of 4 V | 1492 A | External short-circuit resistance of 5 mΩ. <i>SoC</i> of the cell at 100 %. |
|  Smith et al. [2009] | 16 x 18650 lithium-ion cells in parallel. | 280 A | 10 mΩ short-circuit resistance. Drastic fall after 10 s is due to the series <i>PTCs</i> . |
|  Yang et al. [2020] | NCM 18650 2.5 Ah | 135 A | Short-circuit resistance of less than 5 mΩ. <i>SoC</i> of the cell at 85 %. |

Chapter 5

Review of Calculation Methods of Battery Systems External Short-Circuit Currents

“Methods for protection and short-circuit calculation of DC systems are not well established.” Statements like this one are relatively common in the scientific literature of the last thirty years. Berizzi et al. [1994] affirmed that procedures for the calculation of DC short-circuit currents were not well established in the literature. According to Das [2012], although simplified procedures were documented in some publications, DC short-circuit current calculations should be rigorously verified by detailed computer simulations. Similarly, Alho et al. [2018] affirmed that unlike in AC systems, design guidelines for protecting DC systems were still not well established. Satpathi et al. [2019], for instance, stated that despite the advantages provided by DC grids, “the lack of systematic transient analysis and design of comprehensive short-circuit protection algorithms for the full-fledged dc marine vessels have been the major drawbacks for its widespread adoption.”

In this chapter, we perform a review of available methods and procedures for short-circuit current calculations in large battery systems. Relevant papers on smaller battery systems, as well as on DC system protection and fuses, are also mentioned. The sections are organized, as much as possible, in a chronological order to give the reader an idea of how little the methods changed throughout the decades.

5.1 GE Data Book [1958] – Section 173

Although the Sea Zero project deals with lithium-ion batteries, it is worth investigating the methods and procedures developed for lead-acid and nickel-cadmium batteries as well. Therefore, we start with a set of guidelines published in a GE Data Book [1958]. In this data book, at Section 173 “Short-circuit Characteristics of Lead-acid Storage Batteries”, an example of a short-circuit current calculation for a battery system with 60 series-connected lead-acid cells is presented.

The model used in GE Data Book [1958] is the OCV behind an impedance illustrated previously in figure 2.1. However, the pair $R_1 C_1$ is omitted. The system is modeled with the cells’ series resistance R_0 , the external R_s and L_s , and the OCV. The cells themselves are considered to have no internal inductance, i.e., $L_b = 0$. The model used in GE Data Book [1958] is represented by equation (5.1).

$$(R_0 + R_s) i(t) + L_s \frac{di(t)}{dt} = V \quad (5.1)$$

Notice that R_0 , R_s , L_s , and V are constant. The only variables are the time t and the current i .

The solution for the current in the time domain for equation (5.1) is given by

$$i(t) = \frac{V}{R_0 + R_s} (1 - e^{-t/\tau}). \quad (5.2)$$

At $t = 0$ s, the short-circuit fault happens. The pre-fault current supplied or absorbed by the battery is disregarded. The time constant τ , the initial rate of change di/dt , and the peak short-circuit current are given, respectively, by

$$\tau = \frac{L_s}{R_s + R_0}, \quad \frac{di}{dt}(t=0) = \frac{V}{L_s}, \quad \text{and} \quad i_p = \frac{V}{R_s + R_0}.$$

GE Data Book [1958] suggests using AC cable data sheets to find reactance per meter values and then divide them by the cable's rated angular frequency to obtain inductance per meter. It is also suggested to employ natural logarithmic equations for estimating the inductance of parallel wires with the same diameter carrying currents in opposite directions. Empirical methods to estimate the OCV and R_0 are also recommended.

5.2 Fuses for DC Applications: Where We Stood in 1991 and 1992

In the event of an external short-circuit fault, the battery cells are rapidly discharged. This can cause the cells' electrolyte to heat to the point of ignition leading to thermal runaway and toxic gas release. Electrical protections such as fuses and breakers are the key to prevent catastrophic failures [Helgesen, 2019]. Two papers published in the beginning of the 1990s, one on the protection of battery systems by Nailen [1991] and another one on fuses for protecting DC systems by Brozek [1992], had the wording "where we stand" in their titles. In the following paragraphs, we summarize the point of view from the beginning of the 1990s of these authors.

Nailen [1991], who worked at the Wisconsin Electric Power Co now WEC Group, expressed worries regarding catastrophic damages that could be caused by faults in large battery systems. According to this author, in 1991, MW range 400-500 V batteries were no longer only found in heavy industry facilities, but were also being sold as "maintenance free" solutions for large office complexes. In spite of these system's short-circuit currents being large enough to vaporize large conductors, the methods for protecting them were not yet well established. Nailen stated, for example, that in a 1984 exemplar of the "definitive book" on fuse applications by Wright and Newbery, nearly 200 pages were devoted to "the behavior and application of fuses in all sorts of electric circuits - except battery circuits." We do not, unfortunately, have the same 1984 exemplar as Nailen, but in chapter 7 "Applications of fuses" of the 2004 edition of the book "Electric Fuses" by Wright and Newbery, there is no section dedicated exclusively to battery systems.

Brozek [1992], who worked for Copper Industries Bussmann Division now Eaton, discussed the issues of breaking fault currents with fuses in DC systems with longer time constants $\tau = L/R$. Fuse links are designed with weak spots connected in series that are supposed to begin to melt simultaneously. Silica sand usually surrounds the link and serves as a heat absorbing material. Longer time constants lead to a slower rise of the fault current. This increases the chance that not all weak spots melt simultaneously. Therefore, the first weak spots to melt may be subjected to higher than expected arcing voltages, longer arcing times, and higher heat generation. Remark that the higher τ , the higher the energy that has to be dissipated by the fuse. According to Brozek [1992], a challenging case happens when overloads around 200 % of the fuse's rated current appear in a circuit where the time constant τ is larger than 10 ms. In such cases (in the year 1992), many semiconductor protection fuses would not work properly. "The minimum current required for safely open a semiconductor fuse may range from 2 - 10 times the ampere rating of the fuse." Overload protection should, therefore, be provided by electronic sensing.

5.3 Rules of Thumb for the Peak Current

Different rules of thumb for calculating the peak current supplied by batteries have been suggested along the years. In the following subsections, some of them are discussed.

5.3.1 Twenty-times the Capacity in Ah — Lead-Acid

Hosemann et al. [1992] in a CIGRE session paper described a method of short-circuit current calculation that is identical to the one presented later in IEC 61660-1 [1997]. This method defines two empirical curves, one for the rising time from the beginning of the fault until the peak current and another one for the decaying phase towards a steady-state short-circuit current. When it comes to estimating the peak value of the current, Hosemann et al. [1992] suggested that an empirical method could be used:

“Estimation of the peak value of the battery current may be based upon the capacity; the peak value in amperes is then 20 times the capacity in ampere-hours, e.g. 40 kA for 2000 Ah.”

Hosemann et al. [1992] also present a figure with the external short-circuit current of a lead-acid battery string rated 25.2 V and 1125 Ah. For 100 % SoC, the peak current reaches approximately 20 kA in less than 16 ms. For 62 % SoC (700 Ah), the peak of 12 kA is reached in less than 10 ms. For a low SoC of 6.6 % (75 Ah), the peak of 2 kA is reached within 4 ms. The shape of the short-circuit current at rated SoC is similar to the one shown later in figure 5.2 (page 26) with a rising phase, a peak, and a decaying phase. However, the lower the SoC, the less noticeable the decay phase is.

The rough estimate of multiplying the capacity in Ah by a given number has been questioned along the years. Gunther et al. [2017], for instance, short circuited three different lead-acid strings of 26 V and capacities of 1496 Ah, 1800 Ah, and 2320 Ah. The peak short-circuit currents were 10.90 kA, 12.70 kA, and 13.52 kA, which yielded “rule-of-thumb factors” of 7.29, 7.05, and 5.83, respectively. In addition to these findings, Gunther et al. [2017] also concluded that:

“testing revealed the significance of the overall circuit impedance on the fault current contributions from the battery and battery chargers. Using **an accurate value for the circuit impedance when calculating fault currents is essential for achieving the desired coordination of the associated protect devices to minimize the impact of a fault on safety system operability.**”¹

Another important issue is that the multiplying factor varies for different battery chemistries. In the annex C of IEEE 946 [2020], for example, it is stated that “the short-circuit capability can range between 7 and 50 times the rated Ah capacity” for nickel-cadmium batteries.

5.3.2 Ten Times the 1 min Ampere Rating — Lead Acid

The rule of thumb of multiplying the 1 min ampere rating of lead-acid batteries by ten to estimate the maximum (zero external resistance) short-circuit current is mentioned by Migliaro [2001] and by EPRI TR-100248 [2002]. In the example presented in annex C of IEEE 946 [2020], there is even a note comparing the estimated peak short-circuit current obtained with the OCV divided by the battery internal resistance and the one obtained with this rule of thumb. The values are a good match, 11.111 kA for the OCV divided by R_0 and 11.390 kA for the rule of thumb.

5.3.3 Ten Times Rated — Lithium-Ion

In their technical brochure “Applications for Battery Storage (BESS)”, ABB [2022] stated that:

- “each battery rack can provide short circuit current contribution that is ten times higher than its rated current according to the battery technology.”

The resulting short-circuit current supplied by dozens of battery racks in parallel could be very large. However, the “ten times” rule is only given as a rough estimate and to indicate that “switching devices must be able to withstand such large short circuit current values.”

¹Emphasis given by us.

ON RULES OF THUMB FOR PEAK SHORT-CIRCUIT CURRENTS

- These rules provide rough estimates that allow preliminary assessments of prospective or existing installations, however, they are **too imprecise to be used in the design** of large battery systems.

5.4 Guides and Recommendations from 1997 to 2020

5.4.1 IEEE 399 [1997] — Recommended Practice for Industrial and Commercial Power Systems Analysis (Brown Book)

Chapter 16 of the now inactive IEEE 399 [1997] is dedicated to the analysis of DC auxiliary power systems. A short section of this chapter deals with short-circuit current calculations of battery systems. The method described in IEEE 399 [1997] is the same as the one in GE Data Book [1958], in other words, an equivalent OCV behind an RL impedance. The drafts to the publication of IEC 61660-1 [1997] are discussed within IEEE 399 [1997].

5.4.2 IEC 61660-1 [1997] — Short-circuit currents in d.c. auxiliary installations in power plants and substations — Part 1: Calculation of short-circuit currents

IEC 61660-1 [1997] represents battery systems by an OCV behind an RL impedance as done in GE Data Book [1958]. The pair R_1C_1 is disregarded from the model. All the connections and cables are aggregated into an equivalent series R_s and L_s . The cells themselves are considered to have no internal inductance, however the parameter L_b represents the inductance of the conductors of a cell or a module. If these cell/module inductances are unknown, IEC 61660-1 [1997] recommends to use $L_b = 0.2 \mu\text{H}$ per cell.

The Method — Despite the simple RL modeling approach adopted in IEC 61660-1 [1997], the standard considers that the cells' internal voltages decrease and series resistances increase during the short-circuit. Instead of complicating the simple RL model, IEC 61660-1 [1997] opts for an empirical description of the short-circuit current with two equations, one for the period in which the current rises until the peak and another one for the period in which the current decays.

The method starts by calculating the peak short-circuit current with equation (5.3), where the OCV (V) and series resistance R_0 are obtained from the manufacturer for a fully charged battery and R_s is the equivalent impedance of all cables and connectors. Notice the empirical safety factor of 0.9 employed for the battery series resistance.

$$i_p = \frac{V_{@100\%SOC}}{0.9R_{0@100\%SOC} + R_s} \quad (5.3)$$

If the fully charged open-circuit voltage is not available, then IEC 61660-1 [1997] recommends the use of a safety factor as in equation (5.4) where V_n is the rated OCV of the battery system.

$$i_p = \frac{1.05 V_n}{0.9R_{0@100\%SOC} + R_s} \quad (5.4)$$

After reaching i_p , IEC 61660-1 [1997] considers that the short-circuit current will decay to a “quasi-steady-state” level i_k one second after the beginning of the fault. This current is given by equation (5.5). The decay in the OCV and increase in R_0 are handled by simple safety factors. There are no detailed estimations of the OCV and R_0 behaviors according to SoC and temperature.

$$i_k = \frac{0.95 V_{@100\%SOC}}{1.1R_0 + R_s} \quad (5.5)$$

Notice that, if the fully charged **open-circuit voltage** is not available, then an empirical safety factor is recommended to be used as in [equation \(5.6\)](#).

$$i_k = \frac{0.95 V_n}{1.1R_0 + R_s} \quad (5.6)$$

The next step in the [IEC 61660-1 \[1997\]](#) method involves calculating the factor δ with [equation \(5.7\)](#). The variables in [equations \(5.3\)](#), [\(5.5\)](#), and [\(5.7\)](#) are represented with the names used in [figure 2.1](#), not with the names defined by the standard. As different authors and standards employ different nomenclatures, we opted for harmonizing the symbol names in this report as much as possible. The inductances of all the cables, busbars, and cell connections are concentrated into $L_b + L_s$. The “magic number” T_B in [equation \(5.7\)](#) is assumed as 30 ms. This same value of 30 ms appears also in [Berizzi et al. \[1994\]](#), [IEC 61660-3 \[2000\]](#), and [Das \[2012\]](#).

$$\frac{1}{\delta} = \frac{2}{\frac{0.9R_0 + R_s}{L_b + L_s} + \frac{1}{T_B}} \quad (5.7)$$

The rising part of the short-circuit current is given by [equation \(5.8\)](#) where i_p comes from [equation \(5.3\)](#). The time t_p to reach the peak current and the time constant τ_{rise} are estimated with the factor $1/\delta$ from [equation \(5.7\)](#) and the curves in [figure 5.1](#).

$$i_{\text{rise}}(t) = i_p \frac{1 - e^{-t/\tau_{\text{rise}}}}{1 - e^{-t_p/\tau_{\text{rise}}}} \quad 0 < t < t_p \quad (5.8)$$

[Equation \(5.9\)](#) is employed for describing the decaying short-circuit current for times $t > t_p$. The decay time constant τ_{decay} is adopted as 100 ms. This same value of 100 ms appears also in [Berizzi et al. \[1994\]](#); [Das \[2012\]](#); [IEC 61660-3 \[2000\]](#).

$$i_{\text{decay}}(t) = (i_p - i_k) e^{-\frac{t-t_p}{\tau_{\text{decay}}}} + i_k \quad t \geq t_p \quad (5.9)$$

If the decay current i_k cannot be defined, then $i_p = i_k$ and $t_p = T_k$, where T_k is the duration of the short circuit. This results in [equation \(5.8\)](#) being the only description of the battery system external short-circuit current.

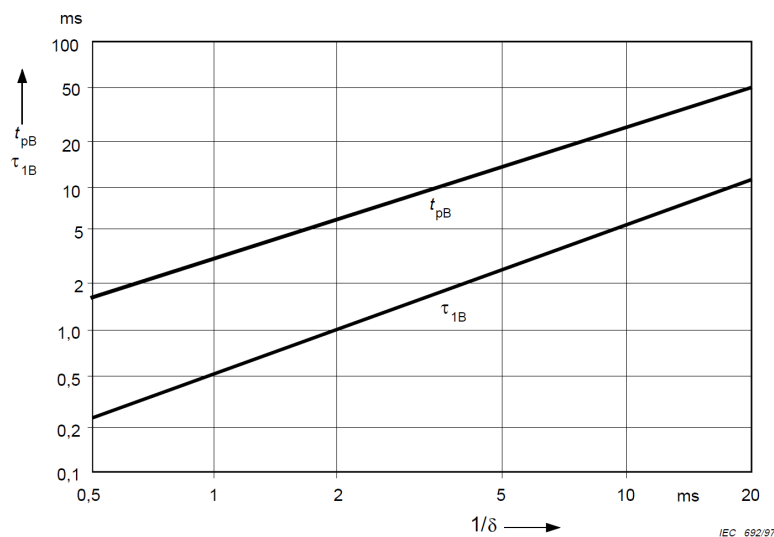


Figure 5.1 | Empirical curves reproduced from [IEC 61660-1 \[1997\]](#) for determining the rise time constant and the time for reaching the peak current. This figure has also been reproduced by [Berizzi et al. \[1994\]](#) and [Das \[2012\]](#). The time constant τ_1 in this figure means τ_{rise} and the time t_{pB} means t_p in [equations \(5.8\)](#) and [\(5.9\)](#), respectively.

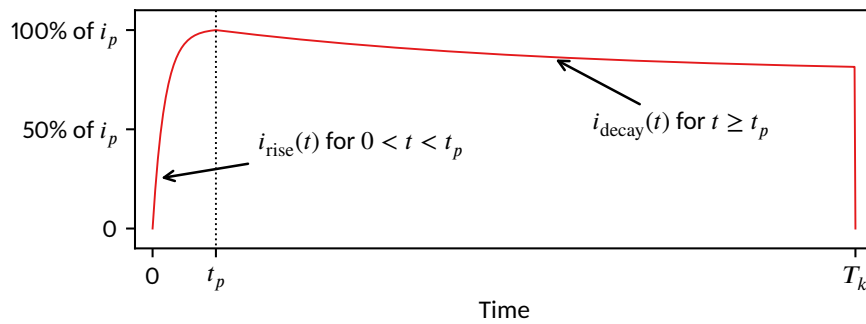


Figure 5.2 | Example of the short-circuit current calculated with equations (5.8) and (5.9).

Figure 5.2 shows an example of short-circuit currents calculated with the method from IEC 61660-1 [1997], in other words, with equations (5.8) and (5.9). Notice that the method starts with parameters from a simple RL circuit, but then uses empirical equations that emulate the results one would obtain if the polarization effects and the dependency on SoC and temperature were taken into consideration. It is worth comparing the shape of the current in figure 5.2 with the one for a short time constant τ_{RC} in figure 2.2b. They feature similar characteristics, but were obtained with different methods. It is important to determine if the approximations and safety factors adopted for equations (5.8) and (5.9) are good enough for lithium-ion batteries. Evaluating the weaknesses and strengths of different short-circuit current calculation methods and assessing their applicability to lithium-ion batteries is one goal of the Sea Zero Project.

ON MAXIMUM AND MINIMUM SHORT-CIRCUIT CURRENTS

In addition to the safety factors assumed for equations (5.8) and (5.9) by IEC 61660-1 [1997], this standard also assumes different conditions for maximum and minimum short-circuit current calculation. For estimating the maximum short-circuit current, the following assumptions are made:

- Conductors are at 20 °C.
- Joint resistances of busbars are neglected.
- Batteries are fully charged. There is no mention to SoH.
- Decoupling diodes are neglected^a.
- Current-limiting effects of fuses must be considered (the standard does not specify how).

The minimum short-circuit current is based on the following assumptions:

- Conductors are at maximum operating temperature.
- Joint resistances of busbars must be considered (with methods provided by the standard).
- Batteries at final discharged voltage as specified by manufacturer (safety factor provided in case this voltage is not available).
- Decoupling diodes have to be considered.
- Current limiting effects of fuses have to be considered.

^aAn example of how decoupling diodes can be used for connecting strings in parallel is shown in C&D [2022].

5.4.3 IEEE 1375 [1998] — Guide for the Protection of Stationary Battery Systems

IEEE 1375 [1998] has a companion standard, namely IEEE 946 [2020], whose full name is “Recommended Practice for the Design of DC Power Systems for Stationary Applications”. The line of demarcation between these two standards is illustrated in figure 5.3.

IEEE 1375 [1998] approaches battery modeling in more detail than the GE Data Book [1958] and IEC 61660-1 [1997]. IEEE 1375 [1998] states, for instance, that the “battery and battery circuit possess a measurable inductance” and that the time constant of the cells themselves, directly between positive and negative terminals, is on the order of 1 to 3 ms which means $L_b > 0$ in figure 2.1. IEEE 1375 [1998] also mentions that the cell polarization effects can be modeled by an R_1C_1 pair with a short time constant and that the effects of this pair for lead-acid and nickel-cadmium batteries last for no more than 15 ms. When it comes to the connecting circuit inductance, IEEE 1375 [1998] states that the total inductive time constant of the battery system including cables and busbars is in the order of 5 to 15 ms. Dependence on SoC and aging are also mentioned in regard to the series resistance R_0 . Furthermore, the variation of the OCV according to SoC for the pre-fault voltage and for the voltage along a prolonged fault are mentioned by IEEE 1375 [1998] as well. Notice, however, that no empirical equations or tables are provided to estimate the OCV and R_0 dependencies.

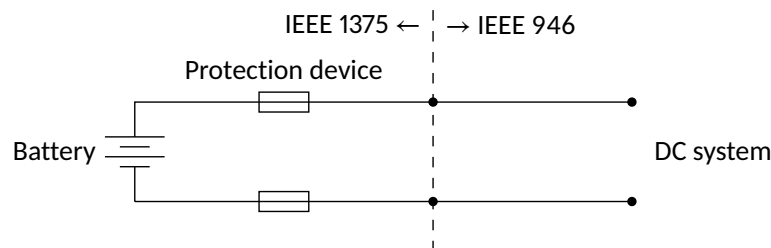


Figure 5.3 | Line of demarcation between IEEE 1375 [1998] and IEEE 946 [2020].

IEEE 1375 [1998] also discusses fuses and circuit breakers for DC systems. The standard suggests simplifying a battery module to a first-order RL circuit with a single time constant τ . This simplification requires the practical measurement of the module’s short-circuit current. See figure 5.4 which was adapted from IEEE 1375 [1998]. In the examples given in the annexes of IEEE 1375 [1998] the battery system and the chargers are reduced to first-order RL circuits. This is done despite earlier mentions to cell polarization effects (R_1C_1), OCV dependency on SoC, and R_0 dependency on SoC and aging. Therefore, when it comes to the practical examples, the simplified battery model adopted by GE Data Book in 1958 is still used in 1998’s IEEE 1375.

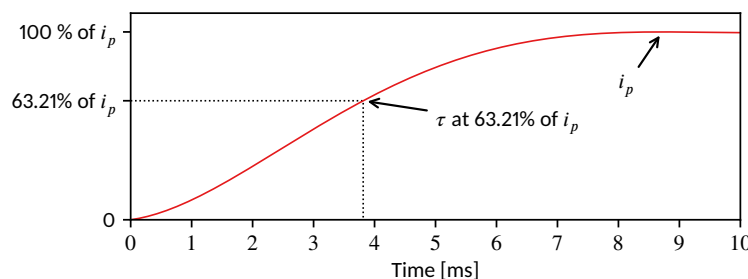


Figure 5.4 | Approximation of the response of the short-circuit current of a module to a first-order RL system with a single time constant τ . The 63.21% rule. Adapted from IEEE 1375 [1998].

ON PARELLEL STRINGS

IEEE 1375 [1998] reminds the designers of battery systems that they “should consider the effects of multiple string short circuits and the effect of a short circuit on an individual string in the parallel system.” The standard also warns designers to “take caution to be aware of the different characteristics of parallel battery string systems from those of single string battery systems.” Nevertheless, the details of selectivity among parallel strings are not discussed by the standard and are considered to be outside the scope of this report.

5.4.4 EPRI TR-100248 [2002] — Stationary Battery Guide: Design, Application, and Maintenance

EPRI TR-100248 [2002] recommends that the simplest way to determine the peak short-circuit current at the terminals of a battery system is to “ask the manufacturer”. However, for quick analyses, the short-circuit current can be estimated as 10 times the 1 minute ampere capability of the cell at 25 °C. This crude method was discussed previously in [section 5.3.2](#).

When it comes to the influence of the inductance seen by the battery during a short-circuit fault, EPRI TR-100248 [2002] states that “a typical stationary battery alone might have a time constant on the order of less than 5 milliseconds at the battery terminals”. If the fault is located further from the battery, “the system time constant might be as high as 15 milliseconds, or longer, depending on the fault location.” The modeling approach suggested for the inductance effect is the first order RL circuit described by [GE Data Book \[1958\]](#).

5.4.5 IEEE 666 [2007] — Design Guide for Electric Power Service Systems for Generating Stations

The now inactive IEEE 666 [2007] discusses briefly, in its section 6.10.1.1, the short-circuit current calculation for battery systems. According to this standard, the battery should be modeled by the series/parallel combination of the battery OCV, battery internal resistances, and the resistance and inductance of all conductors. In summary, the same method described by [GE Data Book \[1958\]](#). The cable impedance depends on the conductor size, length, and composition. Regarding the OCV, the standard recommends that it “should be obtained from the manufacturer and should be the lowest value to which the voltage will drop when the cell is suddenly placed under a heavy load.”

5.4.6 IEEE 946 [2020] — Recommended Practice for the Design of DC Power Systems for Stationary Applications

IEEE 946 [2020] has a companion standard, namely IEEE 1375 [1998], whose full name is “Guide for the Protection of Stationary Battery Systems”, see [section 5.4.3](#). The line of demarcation between these two standards is illustrated in [figure 5.3](#). The annex C of IEEE 946 [2020] presents an example of an external short-circuit current calculation for a battery system. The method is simple and only accounts for the battery equivalent OCV (series and parallel cells), battery equivalent internal resistance (R_0 in [figure 2.1](#) in [page 11](#)), and the total external resistance of cables. The following remarks are interesting to be made regarding the example of short-circuit current calculation presented by IEEE 946 [2020]:

- The estimated bolted short-circuit current (zero external resistance) of one module is 11.111 kA.
- The string short-circuit current considering the equivalent connections, cables, and a 10 mΩ short-circuit resistance is 5.675 kA. In other words, **a drop of almost 50 %** from the maximum possible fault current **because of the external resistances**.

5.5 Selection of Publications that Performed Short-Circuit Faults

In our extensive literature research, we have not found specific standards defining methods for external short-circuit calculations for large lithium-ion battery systems. We have, nevertheless, come across interesting scientific reports and papers on external faults on lithium-ion systems, as well as on systems with other chemistries, that deserve to be commented in this document.

5.5.1 Gerner et al. [2003]: Calculated vs. Measured Short-Circuit Currents

In their white paper, [Gerner et al. \[2003\]](#) compared calculated versus measured short-circuit currents for [valve regulated lead-acid \(VRLA\)](#) batteries rated 12 V with capacities from 33 Ah to 200 Ah. The results of short-circuit tests on an individual 12 V battery are illustrated in [figure 5.5](#). From the test results presented by [Gerner](#)

et al. [2003], we were able to estimate the following characteristics of their battery and short-circuit test rig.

- The OCV (assumed constant during test duration of 50 ms) is 12.4 V.
- Based on the steady-state values of the battery voltage and short-circuit current (after $t = 10$ ms), the external test-rig resistance and the battery internal resistance can be calculated as

$$R_s = \frac{3 \text{ V}}{1.8 \text{ kA}} = 1.67 \text{ m}\Omega \quad \text{and} \quad R_0 = \frac{12.4 \text{ V} - 3 \text{ V}}{1.8 \text{ kA}} = 5.2 \text{ m}\Omega. \quad (5.10)$$

- With the resistances R_0 and R_s and with the time it takes for the short-circuit current to achieve 63% of the steady-state, we can estimate the total inductance of the system as

$$L_b + L_s = \tau_{RL} \times (R_s + R_0) = 2.2 \text{ ms} \times (1.67 \text{ m}\Omega + 5.2 \text{ m}\Omega) = 15.11 \text{ }\mu\text{H}. \quad (5.11)$$

However, **we are not able to distinguish how much of the total inductance belongs to the test rig and how much belongs to the battery.** See in dashed blue in figure 5.5 the results of computer simulations that we performed with the identified parameters in equations (5.10) and (5.11). Our intent with these simulations is to verify if the test results obtained by Gerner et al. [2003] can be reproduced by an impedance-behind-voltage model.

Gerner et al. [2003] stated that the measured external resistance of their test rig was $R_s = 1.8 \text{ m}\Omega$. Given the noisy curves in figure 5.5, we can say that there is a good match between the value of R_s mentioned by the authors and the estimated one with equation (5.10). Notice, however, that the authors did not measure the external inductance L_s nor provided the battery's internal resistance R_0 .

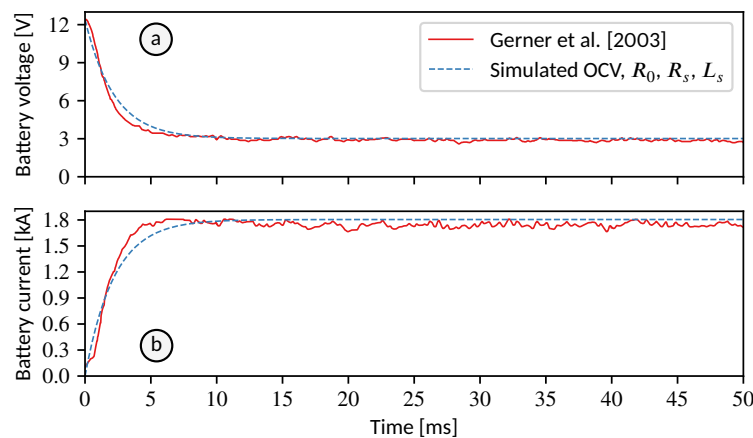


Figure 5.5 | Battery voltage (a) and current (b) during a short-circuit. Acquired with image identification techniques from the original in Gerner et al. [2003] shown in solid red. The results of a computer simulation performed by us with an RL model are shown in dashed blue.

Gerner et al. [2003] also tested a string with $40 \times 12 \text{ V}$ batteries connected in series. This string was protected by a thermal-magnetic molded-case circuit breaker (ABB S3N100TW – 3 pole, 100 A). More details on this test rig can be found in section 6.2. The short-circuit current of the string behaved quite differently from the short-circuit current of one single battery. For the single battery (figure 5.5), the current behavior can be described by a first order RL circuit. However, the behavior of the short-circuit current for the string (figure 5.6) cannot.

The results presented in solid red in figure 5.6 were logged by Gerner et al. [2003] with a sampling time of 0.1 ms. Within this time scale, the rise in the short-circuit current from zero to above 5 kA happens almost instantaneously. Gerner et al. [2003] attribute this spike “to the relative length of cabling for each ‘system’ and

their inductive properties". It is possible, however, to model the observed phenomena by including the pair R_1C_1 from figure 2.1.

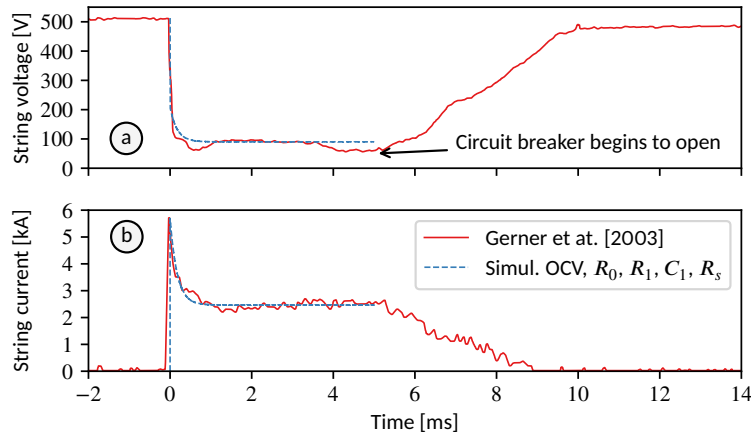


Figure 5.6 | String voltage (a) and current (b) during a short-circuit. Acquired with image identification techniques from the original in Gerner et al. [2003] in solid red. The results of a computer simulation performed by us with RLC model are shown in dashed blue.

The following analysis was performed by us based on the test results provided by Gerner et al. [2003] of a string with forty modules in series (solid red lines in figure 5.6):

- The total equivalent OCV is assumed constant, i.e., $V = 513$ V.
- The total inductance of the system must be close to zero to allow the almost instantaneous rise of the short-circuit current to 5.7 kA, i.e,

$$L_b + L_s \approx 0.$$

We expected the total inductance of a string of 40 cells to be higher than the one observed with only one cell (see equation (5.11)). However, we do not have an **explanation for the inductance of the string being almost zero when the test in one cell indicated a total inductance of 15.11 μ H** (see equation (5.11)).

- The external resistance R_s can be estimated from the quasi steady-state values before the protection circuit breaker begins to open at time $t = 3$ ms:

$$R_s = \frac{90 \text{ V}}{2.47 \text{ kA}} = 36.4 \text{ m}\Omega.$$

Notice how **the total external resistance of the test rig increased considerably** when compared to the case of one single battery in equation (5.10).

- The value of R_0 can be estimated from the peak current at the time of the fault:

$$R_0 + R_s = \frac{513 \text{ V}}{5.7 \text{ kA}} \Rightarrow R_0 = 53.6 \text{ m}\Omega.$$

- The value of R_1 can be estimated from the OCV and the string voltage at $t = 3$ ms:

$$R_1 = \frac{513 \text{ V} - 90 \text{ V}}{2.47 \text{ kA}} - R_0 = 118 \text{ m}\Omega.$$

- Assuming that the decay in the current from time zero to 3 ms is only determined by the time constant τ_{RC} , then the capacitance C_1 can be estimated as:

$$\tau_{RC} = R_1C_1 \Rightarrow C_1 = \frac{0.4 \text{ ms}}{118 \text{ m}\Omega} = 34 \text{ mF}.$$

The results of a computer simulation with the identified V , R_0 , R_1 , C_1 , and R_s are shown in dashed blue in figure 5.6. There is a good match between our computer simulation and the measured values by Gerner et al. [2003]. It is worth emphasizing that we still have **no explanation for the identified inductance of the string being almost zero while the total inductance identified for one module was not.**

5.5.2 Smith et al. [2009]: Sixteen 18650 Lithium-ion Cells Connected in Parallel

In a paper on “Thermal/electrical modeling for abuse-tolerant design of lithium ion modules”, which borrows from an extensive NASA report [Manzo, 2008], Smith et al. [2009] show the results of external short-circuit faults applied to sixteen 18650 lithium-ion cells connected in parallel. Each of these cells has an internal series connected PTC element that increases its resistance drastically after a certain temperature threshold is crossed. The purpose of these elements is to limit the external short-circuit current once the cell reaches a given temperature avoiding thermal runaway.

The model employed by Smith et al. [2009] for reproducing with computer simulations the real short-circuit currents measured from the 16-parallel cells was the OCV behind an impedance shown in figure 2.1 with the following adaptations:

- L_b and L_s set to zero (cables and connections of the test rig were short),
- variable OCV depending on SoC,
- variable R_1C_1 and R_0 depending on SoC and temperature,
- and a variable external short-circuit resistance from 10 mΩ to 70 mΩ.

To include the temperature dependency, Smith et al. [2009] built a thermal model for each cell, including their position inside the module. In fact, a considerable part of the paper is dedicated to the thermal modelling and validation. The authors focused on the efficacy and robustness of the PTC elements for limiting short-circuit currents. Notice that, differently from all the standards cited in section 5.4, Smith et al. [2009] **included an R_1C_1 pair in the their battery model.**

5.5.3 Satake et al. [2014]: Guide for DC Breakers

Satake et al. [2014] published a guide for selecting appropriate Fuji Electric DC circuit breakers for protecting against short-circuit and ground faults in photo-voltaic and wind energy systems. In this guide, the authors use an equivalent circuit for the battery system with **an internal OCV, a series resistance R_0 , and two pairs of parallel RC circuits connected in series.** Satake et al. [2014] took the time to match the impedance characteristics of their model in the frequency domain. They presented a chart with the real component of the impedance in the x axis and the imaginary component in the y axis. Although the scale of the axes is not shown, there is a good visual match in the frequency domain between the modeled and measured impedance values. Satake et al. [2014] showed also a chart with the shape of the measured and modeled short-circuit currents. Similarly to the impedance chart, the x and y axes have not units for time nor current. The shape of the currents measured and modeled by Satake et al. [2014], however, match the one illustrated by figure 5.2 in section 5.4.2. It also matches the shape of the modeled short-circuit current with a short time constant $\tau = R_1C_1$ shown in figure 2.2 in page 12.

5.5.4 Gunther et al. [2017]: Tests on Lead-Acid Strings

Gunther et al. [2017] show the results of actual short-circuit tests performed with three different lead-acid strings of 26 V each and capacities of 1496 Ah, 1800 Ah, and 2320 Ah. The authors show curves of real short-circuit faults performed on a test rig, see more on this rig on section 6.4. Figure 5.7 illustrates the results of the short-circuit test performed by Gunther et al. [2017] on the string rated to 2320 Ah. This string has 12 cells in series. The inset of figure 5.7 shows the detail of the first 100 ms of the short-circuit transient. Gunther

et al. [2017] took the time to match these initial responses to a simple model with an OCV behind an RL impedance. It is important to remark that the shape of the current in figure 5.7 for the whole transient is similar to the example calculated with IEC 61660-1 [1997] shown in figure 5.2. Contrary to the observations by Gerner et al. [2003] with a string of 40 VRLA batteries in series, the results obtained by Gunther et al. [2017] show no indication of a sharp spike in initial short-circuit current.

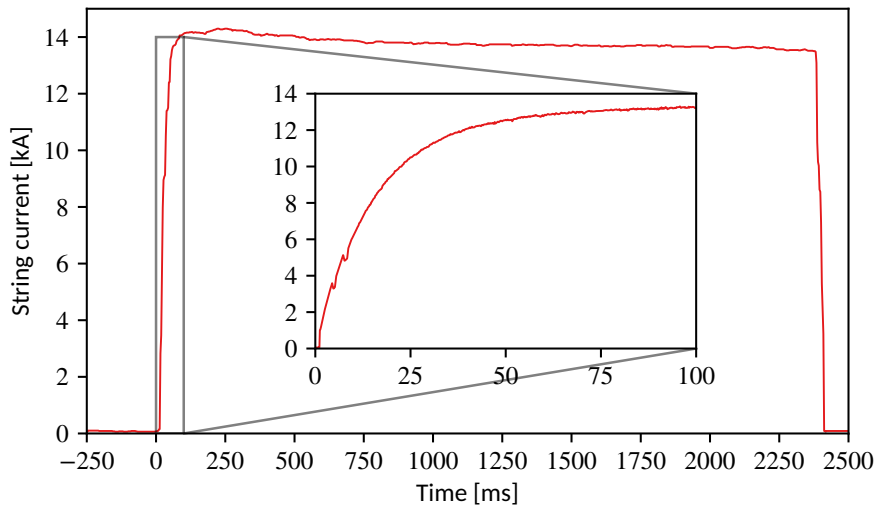


Figure 5.7 | Short-circuit current for a string of lead-acid batteries. Inset shows the detail of the first 100 ms after the fault. String rated to 26 V and 2320 Ah. Data acquired with image identification techniques from the original in Gunther et al. [2017]

5.5.5 Kriston et al. [2017]: Destructive Tests of Lithium-Ion Pouch Cells

Kriston et al. [2017] performed destructive tests in lithium-ion 10 Ah pouch cells. These authors were interested in the thermal evolution of lithium-ion cells subjected to long term short circuits. Most of their short-circuit tests lasted for more than 100 s and were monitored with thermal cameras until the cells began to rupture, vent, or leak electrolyte. Kriston et al. provided charts with logarithmic time scales. Therefore, the initial milliseconds of the short-circuit tests could be visually assessed. Figure 5.8 shows the results, obtained with image identification techniques, from the short-circuit tests of lithium-ion pouch cells.

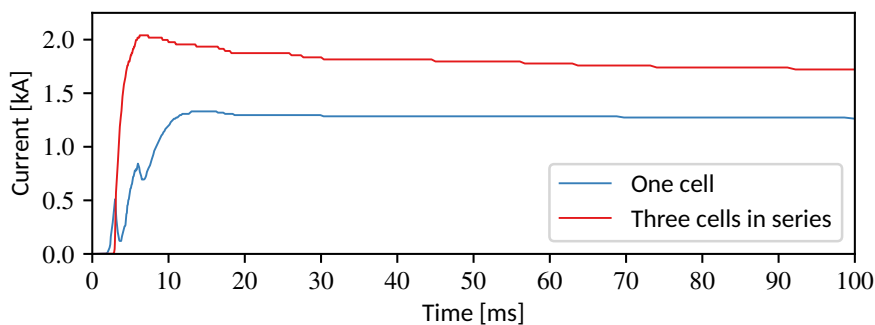


Figure 5.8 | Short-circuit current for 10 Ah pouch cells. Single-cell test in blue. Three cells in series in red. Data acquired with image identification techniques from the original in Kriston et al. [2017]

From the data and charts presented by Kriston et al. [2017], the following analysis can be performed:

- Cells' OCVs: $V = 4$ V.

- Series resistance (R_0) and total external resistance (R_s):
 - Single cell: $R_0 = 1.0 \text{ m}\Omega$; $R_s = 1.3 \text{ m}\Omega$.
 - Three cells: $R_0 = 1.0 \text{ m}\Omega$, $1.0 \text{ m}\Omega$, and $0.9 \text{ m}\Omega$; $R_s = 1.1 \text{ m}\Omega$.

Kriston et al. did not explain how R_0 was measured. They did not explain either why the total external resistance (R_s) for one single cell was lower than the one for three cells connected in series. One would expect the extra connections between the three cells would increase the total external short-circuit resistance.

- Roughly expected peak short-circuit current:
 - Single cell: $i_p = \frac{4 \text{ V}}{2.3 \text{ m}\Omega} = 1.74 \text{ kA}$. Three cells: $i_p = \frac{12 \text{ V}}{4 \text{ m}\Omega} = 3 \text{ kA}$.

The roughly calculated peak currents are considerably higher than the ones observed during the tests (figure 5.8). Based on this fact, and also on the shapes of the currents, one can conclude that a more detailed equivalent circuit model of the cells might be necessary ($R_1 C_1$, for instance) for properly estimating fault currents. Another possibility is that the total external short-circuit resistance of the test setup is, in fact, larger than the value informed by the authors.

ON CONTACTOR HICKUPS

- There are two initial spikes in the short-circuit current supplied by the single 10 Ah cell short-circuit (blue) in figure 5.8. According to Kriston et al. [2017], these spikes are due to “the **bouncing of the copper bar contactor**^a of the short circuit test equipment after closure.”
- Contactor hiccups as the ones observed in Kriston et al. [2017] hinder proper conclusions about the initial milliseconds after the fault. They may also invalidate attempts to scale the results obtained with reduced tests up to a complete large battery system.

^aEmphasis given by us.

5.6 On State of Charge

As discussed in several passages of this report, the current provided by a battery system to an external short-circuit fault depends on the battery’s SoC. Before concluding this section, it is worth discussing practical results available in the literature of lithium-ion batteries short circuit tests at different SoC levels.

Xia et al. [2014] performed long-term short circuit tests in single 18650 cylindrical cells with the SoC varying from zero to 100 % in steps of 10 %. The most noticeable differences in the short-circuit happen a few seconds after the fault. The cells with SoC equal to and above 30 % feature peaks between 60 A and 70 A that drop to a plateau around 30 A within 10 s. The overall shape of the short-circuit current, with peak and plateau, is similar to the one shown previously in figure 4.2 for Yang et al. [2020]. The cells tested with SoC equal to and below 30 % feature a similar peak, but the short-circuit current drops almost exponentially to zero without the previously observed plateau. Xia et al. employed a long sampling time of 100 ms. It is, therefore, impossible to draw conclusions concerning the current rise in the first milliseconds after the fault.

Chen et al. [2016] performed external short-circuit tests in ten 18650-type lithium cells at SoCs varying from 10 % to 100 %. The focus of Chen et al. was to identify external short-circuit faults to the cells employed in electrical vehicle battery packs. The authors’ method, which is insensitive to the battery’s SoC, could identify such a fault within 5 s. Unfortunately, the charts provided by Chen et al. represent the initial milliseconds after the fault as almost vertical straight lines. It is, nevertheless, worth comparing the peak currents achieved within 200 ms of the faults:

- $80 \% \leq \text{SoC} \leq 100 \%$: peaks between 70 A and 75 A,
- $20 \% \leq \text{SoC} \leq 70 \%$: peaks between 60 A and 70 A,
- $\text{SoC} = 10 \%$: peak at 52 A.

Similarly to the results obtained by Xia et al. [2014], Chen et al. [2016] also observed that the most noticeable difference in the peak short-circuit current within 200 ms of the fault is observed for the extremely low SoCs.

As a conclusion to the discussion on the peak short-circuit current versus SoC, we would like to quote Jung et al. [2022]:

“From the test results for the short-circuit resistance of 30 mΩ, it is found that the variations in the magnitude of the current and temperature, depending on the SoC conditions, are insignificant and the current and temperature profiles for both the prismatic and pouch-type batteries are similar in their trends.”

ON SOC VERSUS PEAK EXTERNAL SHORT-CIRCUIT CURRENTS FROM LITHIUM-ION CELLS

- Jung et al. [2022]: SoC does not have significant impact in short-circuit currents (for the short-circuit resistance of 30 mΩ).
- Chen et al. [2016]; Xia et al. [2014]: the most noticeable differences appeared at very low SoC.

Chapter 6

Short-Circuit Test Rigs

The proper validation of a method for the calculation of the external short-circuit current supplied by a battery system demands, invariably, a form of real-life testing. Depending on the size of the battery system available to those who propose a method, the tests are performed in reduced-scale rigs or with the complete real-life system. In our research on methods for short-circuit current calculation for battery systems, we found similar test rigs employed by different authors. In the following sections, we will describe a few relevant examples. Notice that we did not reproduce the original figures from the scientific papers and industry reports.

6.1 Simple Rigs for Testing Single Cells

Authors that investigate external short-circuit faults in single lithium-ion cells tend to opt for simple test rigs, which usually feature:

- one single cell under test,
- one power switch,
- short cables and connecting devices,
- one current measurement shunt.

In many cases, authors do not specify any of the cables, connecting devices, and power switches they used. For instance, in their study on external short-circuit diagnosis, [Xia et al. \[2014\]](#) did not show pictures of their test rig nor specified the types of the contactor and cables. [Xia et al.](#) only mentioned the total external resistance, which was 3.3 mΩ. Another example of succinct descriptions without detailing components was given by [Chen et al. \[2016\]](#), which state that their “lithium cell, relay, and sensors are placed in a safety protection box while the safety protection box is placed in the temperature control box. The relay module is driven by the... controller to close, connecting the positive and negative terminals of the cell through a 25 mΩ wire.” Other authors, however, choose to describe in more detail their test rigs. For example, in their study of the influence of the external short-circuit resistance, [Abaza et al. \[2018\]](#) showed a picture of their rig that was composed of short connection cables, a 24 μΩ shunt resistor, and a power contactor. Notwithstanding, [Abaza et al.](#) did not inform the type or make of the power contactor employed for short-circuiting the battery.

6.2 String of VRLA batteries — [Gerner et al. \[2003\]](#)

In their white paper, [Gerner et al. \[2003\]](#) showed the results of short-circuit tests performed in single VRLA batteries and in strings with 40 batteries in series. [Figure 6.1](#) illustrates the test rig employed by [Gerner et al. \[2003\]](#). It is important to remark that the authors only described their test rig and did not show any diagram or picture of it. Therefore, [figure 6.1](#) shows our interpretation of the authors’ descriptions in the white paper. The short-circuit fault is closed with the “pressurized bolt switch”, but is opened by the 3-pole protection circuit breaker.

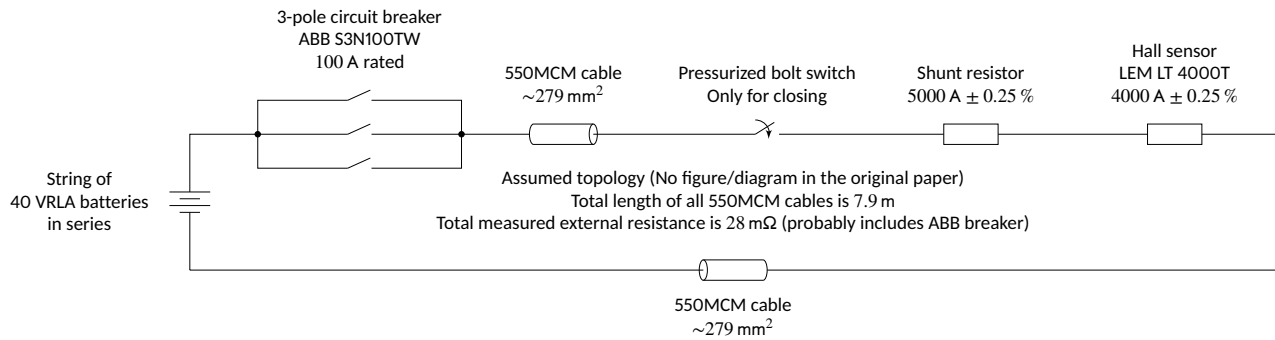


Figure 6.1 | Test rig for short-circuiting a string of 40 VRLA batteries in series used by Gerner et al. [2003]. The diagram is based on our interpretation of the authors' description of the rig.

6.3 Automotive Cells — Conte et al. [2009]

Conte et al. [2009] tested automotive cells up to 60 Ah with peak measured short-circuit currents up to 6 kA. Figure 6.2 shows a diagram illustrating the test rig employed by the authors. Although the paper shows a picture and a diagram of the test rig, the data for the devices and cables are not provided. However, the following guesses can be made:

- the cables seem to be stranded single-core (maybe 95 mm²);
- the picture of the rig seems to show the rear view of a three-pole air circuit breaker similar to a Siemens 3WL or an ABB SACE.

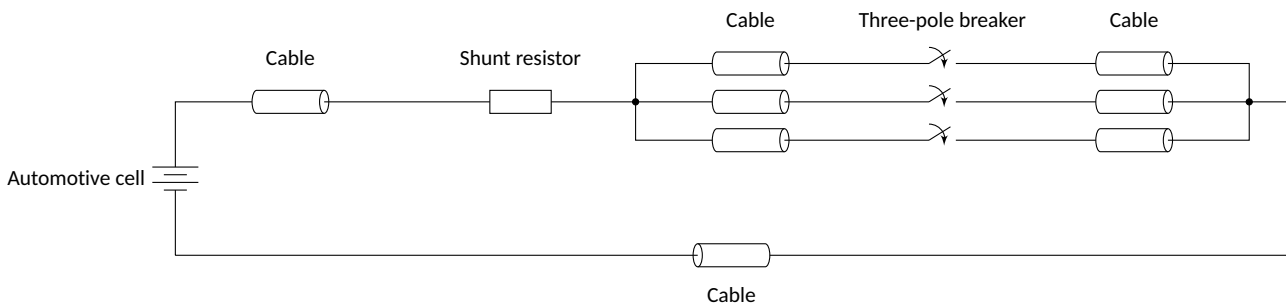


Figure 6.2 | Test rig for one automotive cell used by Conte et al. [2009]. Cables, shunt, and the circuit breaker are not specified by the authors in the paper.

6.4 Large Lead-Acid Strings — Gunther et al. [2017]

In their report on short-circuit currents in DC auxiliary systems in nuclear power plants, Gunther et al. [2017] tested three different strings made of twelve lead-acid cells connected in series. Figure 6.3 shows a diagram of the test rig employed by these authors. For one of the strings tested by the authors, two groups of cells were connected in series by two non-specified inter-tier cables. Each group was composed of six cells connected in series by metallic bars.

During the tests performed by Gunther et al. [2017], the following measurements were acquired:

- voltage across one cell;
- voltage across the whole string;

- voltage at the shunt resistor;
- temperature of the test rig with an infrared camera.

The external temperature of the rig devices measured during the short-circuit tests with the infrared camera, even for the unspecified inter-tier cables, stayed below 33 °C.

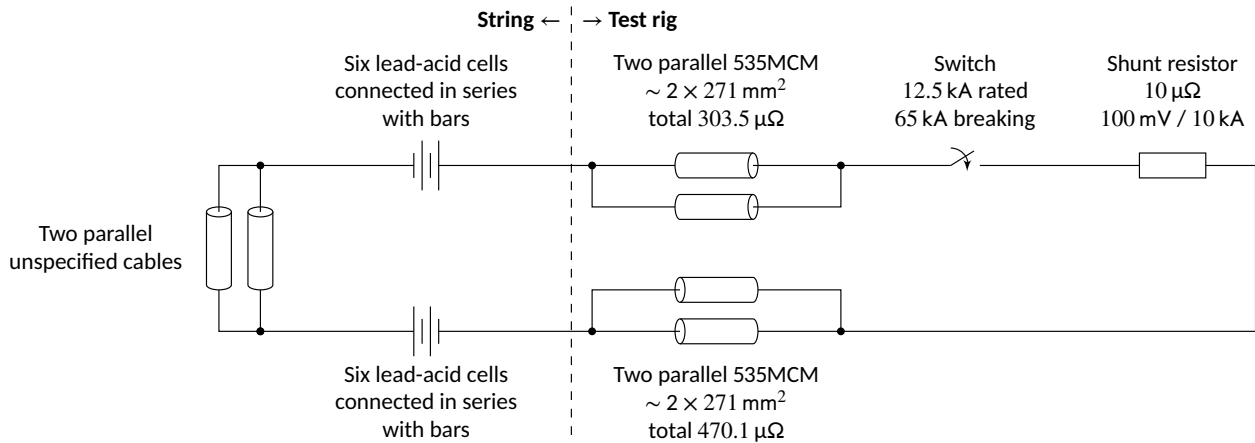


Figure 6.3 | Test rig for twelve lead-acid cells connected in series used by Gunther et al. [2017].

6.5 Variable External Short-Circuit Resistance — Jung et al. [2022]

Jung et al. [2022] studied the influence that the external resistance has on the shape of the short-circuit current of lithium-ion cells. These authors concluded that the required external-short circuit resistances by current standards, among them IEC 62619 [2022] which is described in section 3.1.1, are too high.

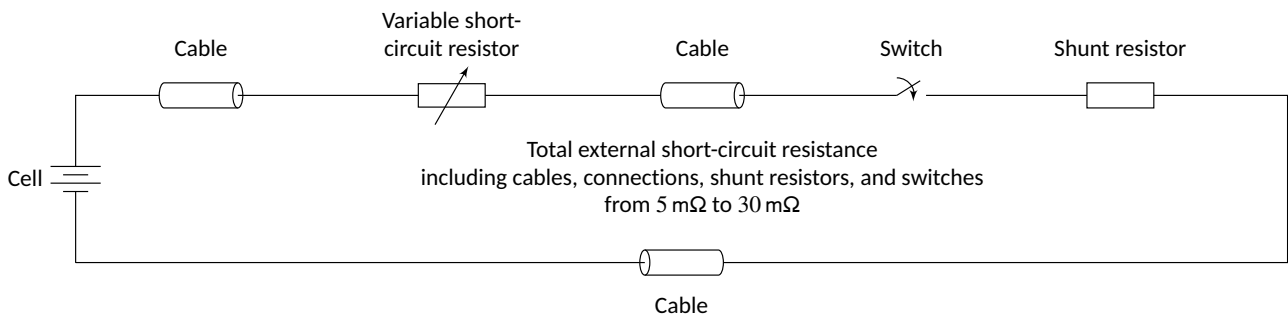


Figure 6.4 | Test rig for lithium-ion cells used by Jung et al. [2022].

Figure 6.4 shows a diagram of the test rig employed by Jung et al. [2022]. The authors did not specify data for the cables, variable resistor, shunt resistor, and short-circuiting switch. However, they did show a picture of the variable resistor which was made of elements connected to each other in series. To adjust the resistance, one needed to reconnect the cable to the different tap positions, see illustration in figure 6.5.

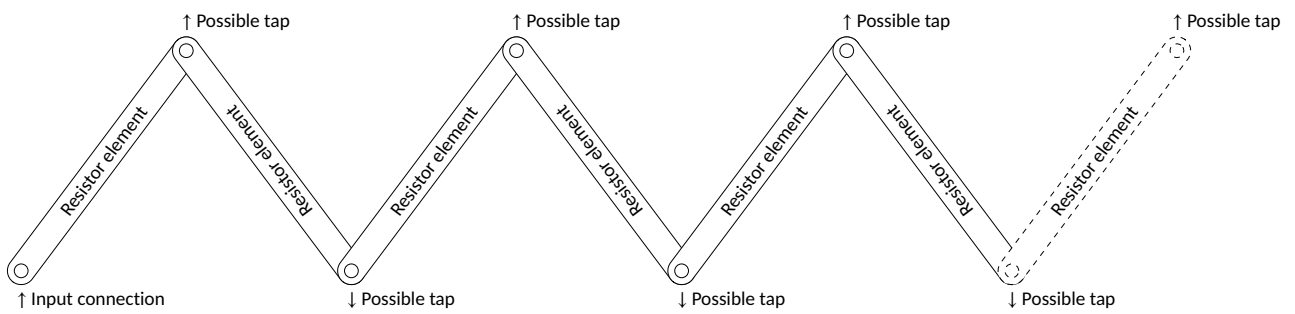


Figure 6.5 | Diagram of the variable external short-circuit resistor employed by Jung et al. [2022].

Chapter 7

Conclusion

In this report, we classified the methods available in the scientific literature for calculating the current provided by large battery systems to external short-circuit faults into three categories, namely:

- (1) electric-equivalent models that represent the whole battery system as an aggregated **OCV** behind an impedance;
- (2) empirical equations that use the aggregated **OCV** and impedance characteristics of the whole battery system for describing the rising and decaying phases of the short-circuit current;
- (3) analytical methods based in different time scales that feature, for instance, electrochemical kinetics and transport phenomena, thermal modeling, and multi-physics coupled models.

The scientific literature on this third category is extensive. However, it is impractical for calculating external short-circuit currents of large battery systems as it tends to focus on investigating dynamics of individual cells, internal short-circuits, thermal runaway dynamics, and new chemistries or materials.

Both methods (1) and (2) named previously rely on estimating electric-equivalent parameters for the whole battery system. The level of detail with which the system is modeled varies among different authors. In many cases, only simple resistive-inductive elements were employed. In other cases, parallel resistive-capacitive elements were considered. Temperature and **SoC** dependency were also taken into account by some authors. Results of actual short-circuit tests presented in the scientific literature were digitized with image identification techniques, plotted, and analyzed in this report. In many cases, simple resistive-inductive impedance models were able to reproduce the results obtained with actual short-circuit tests of strings of battery cells connected in parallel or in series. However, in one notable case, the models obtained from tests with one single battery module could not be matched to the results obtained with a string of forty modules in series. This indicates that the phenomena occurring in long strings of cells in series may not be properly captured by tests with one single cell or module. During the *Sea Zero* project, it will be necessary to evaluate if tests of shortened or even complete battery strings might be required.

The validation of a method for calculating the current supplied by a large battery system to an external short-circuit fault demands, invariably, a form of real-life testing. As a part of the *Sea Zero* project, a laboratory setup for testing individual building blocks or reduced versions of a large battery system will be built. For these reasons, a chapter of this document was dedicated to describing relevant laboratory setups employed by different authors in the scientific literature. The characteristics of the *Sea Zero* test rig will have to be rigorously determined encompassing the impedances of circuit breakers, fuses, cables, connections, and current measurement shunts.

As a concluding remark, we reiterate a relatively common statement present in the scientific literature during the last three decades: “*methods for protection and short-circuit calculation of DC systems are not well established.*” Therefore, within the *Sea Zero* project, a thorough approach will be necessary for properly forecasting fault currents supplied by large battery systems based on the results obtained with laboratory tests of the system’s building blocks. In addition to the proper scaling and matching the laboratory test rigs, special attention will have to be given to large scale phenomena that might not be fully observable in small scale tests.

Abbreviations and Acronyms

The abbreviations and acronyms used in this report are listed below.

| | | |
|-------|--|--|
| AC | Alternate current. | 21, 22 |
| CIGRE | <i>Conseil international des grands réseaux électriques</i> , International Council on Large Electric Systems. | 23 |
| CPE | <i>Constant phase element</i> . | 11, 18 |
| DC | Direct current. | 3–5, 7–9, 19, 21, 22, 24, 27, 31, 36, 39 |
| EES | Electrical energy storage. | 14 |
| ESS | Energy storage system. | 19 |
| EV | Electrical vehicle. | 19 |
| NASA | National Aeronautics and Space Administration. | 31 |
| OCV | Open-circuit voltage. | 11–13, 20–25, 27–32, 39 |
| PTC | Positive temperature coefficient resistor. | 13, 19, 20, 31 |
| PV | Photo-voltaic. | 13 |
| SoC | State of charge. | 5, 7, 11, 13, 14, 18, 20, 23, 24, 26, 27, 31, 33, 34, 39 |
| SoH | State of health. | 7, 11, 26 |
| VRLA | Valve regulated lead–acid. | 4, 28, 32, 35, 36 |

Bibliography

- Abada, S., Marlair, G., Lecocq, A., Petit, M., Sauvant-Moynot, V., and Huet, F. Safety focused modeling of lithium-ion batteries: A review. *Journal of Power Sources*, 306:178–192, February 2016. ISSN 0378-7753. doi: 10.1016/j.jpowsour.2015.11.100. URL <https://www.sciencedirect.com/science/article/pii/S037877531530598X>. Cited on page(s) 10, 19.
- Abaza, A., Ferrari, S., Wong, H. K., Lyness, C., Moore, A., Weaving, J., Blanco-Martin, M., Dashwood, R., and Bhagat, R. Experimental study of internal and external short circuits of commercial automotive pouch lithium-ion cells. *Journal of Energy Storage*, 16:211–217, April 2018. ISSN 2352-152X. doi: 10.1016/j.est.2018.01.015. URL <https://www.sciencedirect.com/science/article/pii/S2352152X16302833>. Cited on page(s) 19, 35.
- ABB. Applications for Battery Storage (BESS). E-Brochure 9AKK108466A8543 Rev A, ABB, May 2022. URL <https://search.abb.com/library/Download.aspx?DocumentID=9AKK108466A8543&LanguageCode=en&DocumentPartId=&Action=Launch>. Cited on page(s) 23.
- Alho, J., Lana, A., Lindh, T., Pyrhönen, O., and Järveläinen, T. Analysis on Short-Circuit Protection in a Battery-Powered Marine Vessel with a DC Distribution System. In *2018 20th European Conference on Power Electronics and Applications (EPE'18 ECCE Europe)*, pages P.1–P.10, Riga, Latvia, September 2018. ISBN 978-90-75815-28-3. URL <https://ieeexplore.ieee.org/document/8515429>. Cited on page(s) 21.
- Berizzi, A., Silvestri, A., Zaninelli, D., and Massucco, S. Short-circuit current calculations for DC systems. In *Proceedings of 1994 IEEE Industry Applications Society Annual Meeting*, volume 2, October 1994. doi: 10.1109/IAS.1994.377744. Cited on page(s) 13, 21, 25.
- Brozek, J. P. DC overcurrent protection - Where we stand. In *Conference Record of the 1992 IEEE Industry Applications Society Annual Meeting*, pages 1306–1310 vol.2, Houston, TX, USA, October 1992. IEEE. doi: 10.1109/IAS.1992.244268. Cited on page(s) 3, 22.
- C&D. Parallel Operation of Lead Acid Batteries. White Paper 41-7952/0112/CD, C&D Technologies, Horsham, PA, USA, 2022. URL https://assets.ctfassets.net/3inf9wk05c1h/2QmQgWYNgcYXcVx6QHxv/c08a152d41228357f6f6a79651029b71/202212-41-7952_Parallel_Operation_Jan2012__1_.pdf. Cited on page(s) 26.
- Chen, Z., Xiong, R., Tian, J., Shang, X., and Lu, J. Model-based fault diagnosis approach on external short circuit of lithium-ion battery used in electric vehicles. *Applied Energy*, 184:365–374, December 2016. ISSN 0306-2619. doi: 10.1016/j.apenergy.2016.10.026. URL <https://www.sciencedirect.com/science/article/pii/S0306261916314507>. Cited on page(s) 10, 13, 33, 34, 35.
- Conte, F. V., Gollob, P., and Lacher, H. Safety in the battery design: the short circuit. *World Electric Vehicle Journal*, 3(4), December 2009. ISSN 2032-6653. doi: 10.3390/wevj3040719. URL <https://www.mdpi.com/2032-6653/3/4/719>. Number: 4 Publisher: Multidisciplinary Digital Publishing Institute. Cited on page(s) 4, 17, 18, 19, 20, 36.
- Das, J. C. Arc Flash Hazard Calculations in DC Systems. In *ARC Flash Hazard Analysis and Mitigation*, pages 503–539. IEEE and John Wiley & Sons, USA, first edition edition, 2012. ISBN 978-1-118-40246-7. doi: 10.1002/9781118402498.ch15. URL <https://ieeexplore.ieee.org/document/6307948>. Cited on page(s) 21, 25.
- DNV-RU-SHIP Pt.6 Ch.2. Part 6 Additional Class Notations Chapter 2 Propulsion, Power Generation and Auxiliary Systems. Rules for Classification Ships DNV-RU-SHIP Pt.6 Ch.2. Edition July 2022, DNV AS, Oslo, Norway, July 2022. Cited on page(s) 3, 14, 15, 16, 17.
- EPRI TR-100248. Stationary Battery Guide: Design, Application, and Maintenance:. Technical Report -Nuclear Maintenance Application Center Revision of TR-100248 1006757, Electric Power Research Institute, Inc (EPRI), Palo Alto, CA, USA, August 2002. URL <https://www.epri.com/research/products/1006757>. Cited on page(s) 3, 23, 28.
- GE Data Book. Industrial Power Systems Data Book. Prepared by System Sales and Engineering Operation, General Electric Company, Schenectady, NY, USA, November 1958. URL https://digital.lib.uiowa.edu/islandora/object/ui:uidb_10896. Cited on page(s) 3, 13, 21, 22, 24, 27, 28.
- Gerner, S. D., Korinek, P. D., and Ruhlmann, T. E. Calculated vs. Actual Short Circuit Currents for VRLA Batteries. White Paper, C&D Technologies, Horsham, PA, USA, 2003. URL <https://www.sbsbattery.com/PDFs/VRLAshortCurrentsStorageBatterySystems.pdf>. The year is actually not stated in the white paper, but it was guessed from the metadata of the PDF file. Cited on page(s) 4, 28, 29, 30, 31, 32, 35, 36.
- Gunther, W., Joshi, P., Celebi, Y., Higgins, J., Weidner, R., and Uhlir, K. Testing to Evaluate Battery and Battery Charger ShortCircuit Current Contributions to a Fault on the DC Distribution System. Report NUREG/CR-7229, United States Nuclear Regulatory Commission, Washington, DC, USA, February 2017. URL <https://www.nrc.gov/docs/ML1703/ML17039A869.pdf>. Cited on page(s) 4, 13, 23, 31, 32, 36, 37.
- Helgesen, H. Technical Reference for Li-ion Battery Explosion Risk and Fire Suppression. Technical Report 1144K9G7-12 2019-1025, Rev. 4, DNV GL, Høvik, Norway, November 2019. Cited on page(s) 9, 22.

- Hosemann, G., Nietsch, C., and Tsanakas, D. Short-circuit stress in DC auxiliary systems. In *Session Materials*, volume 23-104, Paris, France, September 1992. CIGRE. URL https://e-cigre.org/publication/23_104_1992-short-circuit-stress-in-dc-auxiliary-systems. Cited on page(s) 23.
- IEC 61660-1. Short-circuit currents in d.c. auxiliary installations in power plants and substations - Part 1: Calculation of short-circuit currents. International Standard IEC 61660-1:1997, International Electrotechnical Commission (IEC), Geneva, Switzerland, 1997. URL <https://webstore.iec.ch/publication/5700>. Cited on page(s) 3, 10, 13, 23, 24, 25, 26, 27, 32.
- IEC 61660-3. Short-circuit currents in d.c. auxiliary installations in power plants and substations - Part 3: Examples of calculations. International Standard IEC TR 61660-3:2000, International Electrotechnical Commission (IEC), Geneva, Switzerland, 2000. URL <https://webstore.iec.ch/publication/5704>. Cited on page(s) 25.
- IEC 62619. Secondary cells and batteries containing alkaline or other non-acid electrolytes – Safety requirements for secondary lithium cells and batteries, for use in industrial applications. International Standard IEC 62619 Edition 2.0, International Electrotechnical Commission (IEC), Geneva, Switzerland, May 2022. URL <https://webstore.iec.ch/publication/5700>. Cited on page(s) 15, 16, 17, 37.
- IEEE 1375. Guide for the Protection of Stationary Battery Systems. IEEE Std 1375-1998, IEEE, USA, 1998. DOI 10.1109/IEEESTD.1998.87900. Cited on page(s) 3, 13, 26, 27, 28.
- IEEE 399. IEEE Recommended Practice for Industrial and Commercial Power Systems Analysis (Brown Book). IEEE Std, IEEE, USA, August 1997. DOI 10.1109/IEEESTD.1998.88568. Cited on page(s) 3, 24.
- IEEE 45.1. IEEE Recommended Practice for Electrical Installations on Shipboard–Design. IEEE Std 45.1-2017, IEEE, USA, August 2017. DOI 10.1109/IEEESTD.2017.8007394. Cited on page(s) 3, 14, 15, 16.
- IEEE 666. IEEE Design Guide for Electric Power Service Systems for Generating Stations. IEEE Std 666-2007 (Revision of IEEE Std 666-1991), IEEE, USA, May 2007. DOI 10.1109/IEEESTD.2007.357955. Cited on page(s) 3, 28.
- IEEE 946. Recommended Practice for the Design of DC Power Systems for Stationary Applications. IEEE Std 946-2020 (Revision of IEEE Std 946-2004), IEEE, USA, September 2020. DOI 10.1109/IEEESTD.2020.9206101. Cited on page(s) 3, 4, 23, 24, 26, 27, 28.
- Jung, J.-B., Lim, M.-G., Kim, J.-Y., Han, B.-G., Kim, B., and Rho, D.-S. Safety Assessment for External Short Circuit of Li-Ion Battery in ESS Application Based on Operation and Environment Factors. *Energies*, 15(14), January 2022. ISSN 1996-1073. doi: 10.3390/en15145052. URL <https://www.mdpi.com/1996-1073/15/14/5052>. Cited on page(s) 4, 19, 20, 34, 37, 38.
- Kriston, A., Pfrang, A., Döring, H., Fritsch, B., Ruiz, V., Adanouj, I., Kosmidou, T., Ungeheuer, J., and Boon-Brett, L. External short circuit performance of Graphite-LiNi_{1/3}Co_{1/3}Mn_{1/3}O₂ and Graphite-LiNi_{0.8}Co_{0.15}Al_{0.05}O₂ cells at different external resistances. *Journal of Power Sources*, 361:170–181, September 2017. ISSN 0378-7753. doi: 10.1016/j.jpowsour.2017.06.056. URL <https://www.sciencedirect.com/science/article/pii/S037877531730839X>. Cited on page(s) 4, 32, 33.
- Lee, S., Kim, J., Ha, M., and Song, H. Inrush Current Estimation for Hot Swap of the Parallel Connected Large Capacity Battery Pack. In *2018 IEEE Energy Conversion Congress and Exposition (ECCE)*, pages 2489–2492, September 2018. doi: 10.1109/ECCE.2018.8558163. URL <https://ieeexplore.ieee.org/document/8558163>. ISSN: 2329-3748. Cited on page(s) 13.
- Manzo, M. A. NASA Aerospace Flight Battery Program, Part 1 - Volume I, Generic Safety, Handling and Qualification Guidelines for Lithium Ion (Li-Ion) Batteries. Technical Report RP-08-75, NASA, USA, July 2008. URL [https://www.nasa.gov/pdf/287382main_RP-08-75%2006-069-1%20NASA%20Aerospace%20Flight%20Battery%20Program%20\(Part%20I-Volume%20I\)%20\(FINAL\)\(7-10-08\).pdf](https://www.nasa.gov/pdf/287382main_RP-08-75%2006-069-1%20NASA%20Aerospace%20Flight%20Battery%20Program%20(Part%20I-Volume%20I)%20(FINAL)(7-10-08).pdf). Cited on page(s) 31.
- Migliaro, M. W. Stationary Batteries. In Beaty, W. H., editor, *Handbook of Electric Power Calculations*, chapter 18. McGraw-Hill, New York, third edition, 2001. ISBN 978-0-07-136298-6. URL <https://catedras.facet.unt.edu.ar/sep/wp-content/uploads/sites/20/2020/03/Handbook-of-Electric-Power-Calculations-Beaty.pdf>. Cited on page(s) 23.
- Nailen, R. Battery protection-where do we stand? *IEEE Transactions on Industry Applications*, 27(4), July 1991. ISSN 1939-9367. doi: 10.1109/28.85479. Cited on page(s) 3, 17, 22.
- Plett, G. L. *Battery Management Systems: Battery Modeling Volume 1*. Artech House, Boston USA and London UK, 2015. ISBN 978-1-63081-023-8. Cited on page(s) 11.
- Ramadesigan, V., Northrop, P. W. C., De, S., Santhanagopalan, S., Braatz, R. D., and Subramanian, V. R. Modeling and Simulation of Lithium-Ion Batteries from a Systems Engineering Perspective. *Journal of The Electrochemical Society*, 159(3), January 2012. ISSN 1945-7111. doi: 10.1149/2.018203jes. URL <https://iopscience.iop.org/article/10.1149/2.018203jes/meta>. Cited on page(s) 10.
- Rheinfeld, A., Noel, A., Wilhelm, J., Kriston, A., Pfrang, A., and Jossen, A. Quasi-Isothermal External Short Circuit Tests Applied to Lithium-Ion Cells: Part I. Measurements. *Journal of The Electrochemical Society*, 165(14):A3427, November 2018. ISSN 1945-7111. doi: 10.1149/2.0451814jes. URL <https://iopscience.iop.org/article/10.1149/2.0451814jes/meta>. Publisher: IOP Publishing. Cited on page(s) 10.
- Rheinfeld, A., Sturm, J., Noel, A., Wilhelm, J., Kriston, A., Pfrang, A., and Jossen, A. Quasi-Isothermal External Short Circuit Tests Applied to Lithium-Ion Cells: Part II. Modeling and Simulation. *Journal of The Electrochemical Society*, 166(2):A151, January 2019. ISSN 1945-7111. doi: 10.1149/2.0071902jes. URL <https://iopscience.iop.org/article/10.1149/2.0071902jes/meta>. Publisher: IOP Publishing. Cited on page(s) 10.
- Satake, S., Onchi, T., and Toyama, K. Technology of Estimating Short Circuit Current and Ground Fault for Direct Current Distribution Systems. *Fuji Electric Review* vol. 60 no. 3 2014, Fuji Electric Co., Ltd., Tokyo, Japan, 2014. URL <https://www.fujielectric.com/company/tech/pdf/60-03/FER-60-3-179-2014.pdf>. Cited on page(s) 4, 11, 13, 31.
- Satpathi, K., Ukil, A., Nag, S. S., Pou, J., and Zagrodnik, M. A. DC Marine Power System: Transient Behavior and Fault Management Aspects. *IEEE Transactions on Industrial Informatics*, 15(4):1911–1925, April 2019. ISSN 1941-0050. doi: 10.1109/TII.2018.2864598. Cited on page(s) 21.

- Smith, K., Kim, G.-H., Darcy, E., and Pesaran, A. Thermal/electrical modeling for abuse-tolerant design of lithium ion modules. *International Journal of Energy Research*, 34(2):204–215, December 2009. ISSN 1099-114X. doi: 10.1002/er.1666. URL <https://onlinelibrary.wiley.com/doi/abs/10.1002/er.1666>. Cited on page(s) 4, 13, 19, 20, 31.
- Tremblay, O., Dessaint, L.-A., and Dekkiche, A.-I. A Generic Battery Model for the Dynamic Simulation of Hybrid Electric Vehicles. In *2007 IEEE Vehicle Power and Propulsion Conference*, pages 284–289, September 2007. doi: 10.1109/VPPC.2007.4544139. URL <https://ieeexplore.ieee.org/abstract/document/4544139>. ISSN: 1938-8756. Cited on page(s) 13.
- UN 38.3 T-5. Manual of Tests and Criteria. Seventh revised edition ST/SG/AC.10/11/Rev.7, United Nations, New York, USA and Geneva, Switzerland, 2019. URL https://unece.org/fileadmin/DAM/trans/danger/publi/manual/Rev7/Manual_Rev7_E.pdf. Cited on page(s) 15, 16, 17.
- Wang, B., Li, S. E., Peng, H., and Liu, Z. Fractional-order modeling and parameter identification for lithium-ion batteries. *Journal of Power Sources*, 293:151–161, October 2015. ISSN 0378-7753. doi: 10.1016/j.jpowsour.2015.05.059. URL <https://www.sciencedirect.com/science/article/pii/S0378775315009404>. Cited on page(s) 11.
- Willihnganz, E. and Rohner, P. Battery impedance: Farads, milliohms, microhenrys. *Transactions of the American Institute of Electrical Engineers, Part II: Applications and Industry*, 78(4):259–262, September 1959. ISSN 2379-6774. doi: 10.1109/TAI.1959.6371570. Cited on page(s) 13.
- Wright, A. and Newbery, P. G. *Electric Fuses*. IET Digital Library, 3rd edition edition, 2004. ISBN 978-1-84919-051-0. doi: 10.1049/PBPO049E. URL <https://digital-library.theiet.org/content/books/po/pbpo049e>. Cited on page(s) 22.
- Xia, B., Chen, Z., Mi, C., and Robert, B. External short circuit fault diagnosis for lithium-ion batteries. In *2014 IEEE Transportation Electrification Conference and Expo (ITEC)*, pages 1–7, June 2014. doi: 10.1109/ITEC.2014.6861806. URL <https://ieeexplore.ieee.org/abstract/document/6861806>. Cited on page(s) 18, 20, 33, 34, 35.
- Xia, B., Mi, C., Chen, Z., and Robert, B. Multiple cell lithium-ion battery system electric fault online diagnostics. In *2015 IEEE Transportation Electrification Conference and Expo (ITEC)*, pages 1–7, June 2015. doi: 10.1109/ITEC.2015.7165777. URL <https://ieeexplore.ieee.org/document/7165777>. Cited on page(s) 18.
- Xiong, R., Yang, R., Chen, Z., Shen, W., and Sun, F. Online Fault Diagnosis of External Short Circuit for Lithium-Ion Battery Pack. *IEEE Transactions on Industrial Electronics*, 67(2):1081–1091, February 2020. ISSN 1557-9948. doi: 10.1109/TIE.2019.2899565. URL <https://ieeexplore.ieee.org/document/8648476>. Cited on page(s) 18.
- Yang, R., Xiong, R., He, H., and Chen, Z. A fractional-order model-based battery external short circuit fault diagnosis approach for all-climate electric vehicles application. *Journal of Cleaner Production*, 187:950–959, June 2018. ISSN 0959-6526. doi: 10.1016/j.jclepro.2018.03.259. URL <https://www.sciencedirect.com/science/article/pii/S0959652618309405>. Cited on page(s) 11, 18.
- Yang, R., Xiong, R., Ma, S., and Lin, X. Characterization of external short circuit faults in electric vehicle Li-ion battery packs and prediction using artificial neural networks. *Applied Energy*, 260:114253, February 2020. ISSN 0306-2619. doi: 10.1016/j.apenergy.2019.114253. URL <https://www.sciencedirect.com/science/article/pii/S0306261919319403>. Cited on page(s) 18, 19, 20, 33.
- Zavalis, T. G., Behm, M., and Lindbergh, G. Investigation of Short-Circuit Scenarios in a Lithium-Ion Battery Cell. *Journal of The Electrochemical Society*, 159(6):A848, April 2012. ISSN 1945-7111. doi: 10.1149/2.096206jes. URL <https://iopscience.iop.org/article/10.1149/2.096206jes/meta>. Cited on page(s) 10.
- Zhao, R., Liu, J., and Gu, J. Simulation and experimental study on lithium ion battery short circuit. *Applied Energy*, 173:29–39, July 2016. ISSN 0306-2619. doi: 10.1016/j.apenergy.2016.04.016. URL <https://www.sciencedirect.com/science/article/pii/S0306261916304676>. Cited on page(s) 19.



SINTEF

Technology for a better society